Stony Brook University

A Novel Role for Ciliary Proteins in Zymogen Granule Secretion of Pancreatic Acinar Cells

A Dissertation Presented

by

Benjamin Cyge

to

The Graduate School

in Partial Fulfillment of the

Requirements

for the Degree of

Doctor of Philosophy

in

Molecular and Cellular Pharmacology

Stony Brook University

August 2014

Stony Brook University

The Graduate School

Benjamin Cyge

We, the dissertation committee for the above candidate for the

Doctor of Philosophy degree, hereby recommend

acceptance of this dissertation.

Ken-Ichi Takemaru, Ph. D.
Dissertation Advisor, Associate Professor
Department of Pharmacological Sciences

Gerald H. Thomsen, Ph. D.
Chairperson of Defense, Professor
Department of Biochemistry and Cell Biology

Deborah A. Brown, Ph. D.
Professor
Department of Biochemistry and Cell Biology

Shaoyu Ge, Ph. D.
Associate Professor
Department of Neurobiology and Behavior

Howard C. Crawford, Ph. D.
Associate Professor, Mayo Clinic
Department of Cancer Biology

This dissertation is accepted by the Graduate School

Charles Taber
Dean of the Graduate School

Abstract of the Dissertation

A Novel Role for Ciliary Proteins in Zymogen Granule Secretion of Pancreatic Acinar Cells

by

Benjamin Cyge

Doctor of Philosophy

in

Molecular and Cellular Pharmacology

Stony Brook University

2014

Primary cilia are present on nearly all mammalian cells. For many years, they were thought to be functionless, vestigial organelles. In recent years, primary cilia have been found to be essential for many important biological processes. Included in these are chemo – and mechano-sensation, as well as acting as a signaling hub for hedgehog, Wnt, and notch signaling. Further exemplifying their importance, there is a new classification of genetic disorders, collectively referred to as ciliopathies, which manifest due to aberrant growth and regulation of cilia, and aberrant expression of gene products thought to be critical for these processes. Our lab utilizes a transgenic mouse, which is completely lacking the gene Chibby (Cby). This mutant mouse has been found to have a vast distribution of phenotypes, which overlap with many known ciliopathies. These include chronic sinusitis and otitis, infertility, polycystic kidneys, and pancreatic degeneration. Subsequently, it was found that Cby plays a vital role in ciliogenesis. Of the phenotypes mentioned, the one that has the least mechanistic understanding is pancreatic

degeneration. This phenotype has been characterized in a number of other mouse mutants, which have aberrant expression of ciliary genes. The pancreas is composed of two major subclasses, the exocrine and endocrine tissue. The endocrine tissue is composed of the islets of Langerhans, which help to regulate glucose homeostasis. The exocrine tissue is composed mainly of acinar cells, which produce and secrete digestive enzymes in the form of inactive zymogens. These zymogens are secreted apically into the ductal network, where they are transported to the duodenum to aid in proper digestion. All of the endocrine cells, as well as the ductal cells contain primary cilia. The only cells that do not contain primary cilia are the acinar cells. In these ciliopathy mouse models, the cells most deleteriously affected are the acinar cells, which rapidly degenerate after birth. Because of this phenomenon, it has been previously speculated that these cells are degenerating non-cell autonomously. My work has found this not to be the case. I show that acinar cells in Cby mouse models, as well as at least one of these other models, IFT88, are dying cell-autonomously, and these gene products are expressed in acinar cells and play a vital role in proper zymogen vesicle secretion, and in their absence, acinar cells degenerate rapidly due to improper trafficking and secretion. Collectively my work supports growing evidence that ciliary gene products have vital roles outside of the cilium in membrane trafficking, and collectively referring to any phenotype resulting from aberrant expression of these gene products, as a ciliopathy may be naïve.

Table of Contents

List of Figures

List of Abbreviations

BBS	Bardet-Biedl syndrome
BSA	Bovine serum albumin
Cby	Chibby
Cby KD	Chibby knock down
CP	Chronic pancreatitis
DAPI	4', 6-diamidino-2-phenylindole
DW	Deionized water
FBS	Fetal bovine serum
HBSS	Hank's balanced salt solution
Hh	Hedgehog
IF	Immunofluorescence
IFT	Intraflagellar transport
IPB	Immunoprecipitation buffer
MKS	Meckel-Gruber syndrome
O.C.T.	Optimal cutting temperature
OFD	Oral-Facial-Digital syndrome
PBS	Phosphate buffered saline
PCD	Primary ciliary dyskinesia
PFA	Paraformaldehyde
PKA	Protein kinase A
PKD	Polycystic kidney disease
PMSF	Phenylmethylsulfonyl fluoride
Ptch	Patched
SDS	Sodium dodecyl sulfate
SDS-PAGE	Sodium dodecyl sulfate polyacrylamide gel electrophoresis
Smo	Smoothened
SUFU	Suppressor of Fused
TEM	Transmission electron microscopy
TBS	Tris-buffered saline
TBST	0.1% Tween-20 in Tris-buffered saline
ZG	Zymogen granule

Acknowledgments

I would like to thank many people for their invaluable support in helping me achieve this milestone.

First and foremost, I would like to thank my advisor, Dr. Ken-Ichi Takemaru. Ken had the faith to give me a chance in his lab many years ago, when I was a sophomore with little knowledge or experience in bench science. From the very beginning, Ken has been a fantastic mentor. While providing the guidance I needed, he also gave me confidence in myself, to help me become an independent scientist. I certainly owe any success I've had, and any I may achieve in the future to having the privilege of such a great mentor.

I would also like to thank Dr. Feng-Qian Li. It is not often that one has access to such a brilliant scientist to discuss ideas with at the spur of the moment. Qian has always been available to give a second opinion on my ideas and data, as well as for technical guidance.

I would like to thank my research advisory committee. Dr. Gerald Thomson has been a fantastic resource. He has always been happy and excited to discuss my work and provide valuable feedback. Dr. Deborah Brown and Dr. Shaoyu Ge have been great sources of expertise and have always had great suggestions for solving the toughest challenges. I would also like to thank Dr. Howard Crawford. It has not been easy working on a project in which neither my advisor nor myself were experts. Howard has certainly helped lighten this load with his expertise in the field of pancreas biology. More than this, Howard has been a mentor and a friend, and has always been supportive and encouraging when I most needed it.

I would also like to thank my many colleagues. George Georghiou has been a great friend by my side, step for step, since were undergraduates together, and Burak Derkunt for his friendship and spirited discussions. My lab mates, Dr. Damon Love, Dr. Adaobi Mofunanya, Dr.

Victoria Fischer, Xingwang Chen, Dex-Ann Brown-Grant, and Saul Siller. Lastly my bench mate, Dr. Michael Burke, for never failing to keep the mood in the lab less than chipper.

I certainly would not be where I am today without the assistance of Dr. Styliani-Anna Tsirka. Stella has always had an open door, as much as I'm sure she would have enjoyed shutting it in my face. There was never a problem that Stella couldn't solve. I also have to hank all of the wonderful administrators, Janice Kito, Odalis Hernandez, Melissa Daley, Lynda Perdomo-Ayala, and Beverly Campbell. Things always ran much more smoothly with the prompt assistance of our IT experts, Paul Stern and Ray Taffner.

I do not know where I would be without the constant love and support of my amazing wife, Heather. Heather has always pushed me to be my best in all facets of life. On the days where I was completely overwhelmed, I always felt better knowing that Heather would be there waiting when I got home.

I would like to thank Dr. Gregory Pazour for kindly providing Orpk pancreas tissue and IFT20 antibody. I would also like to thank Dr. Jonathan Eggenshwiler for providing us with Gli2 antibody.

Chapter 1 General Introduction

Cilia

The cilium is a complex organelle with many important biological functions, such as signaling through mechano- and chemo-sensation in primary cilia, and fluid motility regulated by motile cilia (Goetz & Anderson, 2010; Lee, 2011; Oh & Katsanis, 2012; Satir & Christensen, 2008). Primary cilia are present on nearly all mammalian cell types, and have various functions, which are cell and tissue dependent. While they were thought to be functionless, vestigial organelles for a very long time, in recent years they have been found to have many extremely important functions. Structurally, the ciliary axoneme of primary cilia is arranged in a 9 + 0 arrangement, referring to the circular arrangement of 9 microtubule doublets, which are not associated with any further structural support, and are therefore lacking regulated movement (Yamamoto & Kataoka, 1986). As the interest in primary cilia is still young, there are many unknowns with regard to their function, as well as to how they are regulated. However, recent advances have shed light on many important functions of primary cilia. It is well known that primary cilia are an essential component of most mammalian hedgehog signaling (Bishop et al, 2010; Heretsch et al, 2010; Tukachinsky et al, 2010). Briefly, upon hedgehog ligand binding to the ciliary membrane receptor, patched, the smoothened receptor can translocate to the tip of the cilium. Downstream of this, Gli transcription factor, bound to the negative regulator, Sufu, translocates to the tip of the cilia, where it is thought to be activated via unknown mechanisms by Smoothened, allowing it to dissociate from Sufu, where it can then translocate out of the cilia, and into the nucleus where it can activate downstream target genes. While much less is known about cilia and Wnt signaling, it was reported that Wnt signaling is negatively regulated by the primary cilium, as the β-catenin destruction complex is sequestered at the base of the primary

cilia, and when primary cilia are lost, β-catenin can be aberrantly freed from this complex allowing aberrant activation of Wnt signaling (Lancaster et al, 2011).

The axoneme structure of motile or multi-cilia is arranged in what is known as a 9+2 arrangement (Satir, 1965). These numbers specify the 9 microtubule doublets that surround and central pair of microtubule singlets. The central pair of microtubules are associated with the outer pairs via 9 separate radial spokes. The outer microtubule doublets further interact with each other via connection to dynein arms. The rigidity of the radial spokes, along with the regulated movement of the dynein arms, together, confer regulated motility of motile cilia. Motile cilia are typically present in great numbers on a single cell, allowing them to beat in unison in order to carry out their function. The function of motile cilia varies in a tissue-dependent context, but most often they specialize in movement of fluids, such as directional mucous movement carried out by multi-ciliated tracheal cells, leading to their ultimate clearance (EK & Brody, 2013). In specialized cells that have just one or a few motile cilia, these cilia are referred to as flagella, and are utilized in a beating fashion for cellular movement, such as in mature spermatocytes (Lindemann & Lesich, 2010), or in unicellular organisms, such as *Chlamydomonas* (Rosenbaum et al, 1969).

In addition to this, there are context-dependent specialized cilia in mammalian tissues, such as olfactory, taste, and retinal cilia (Kuhlmann et al, 2014; Lee & Cohen, 2013; Wheway et al, 2013). Due to their diversity of functions, it is not surprising that there is a complementing diversity of human pathologies resulting from dysfunctional cilia. These pathologies are collectively referred to as ciliopathies. These disorders include, but are not limited to, Bardet-Biedl syndrome (BBS), Joubert syndrome, Meckel-Gruber syndrome (MKS), polycystic kidney disease (PKD), and primary ciliary dyskinesia (PCD) (van Reeuwijk et al, 2011). While they

share common phenotypes of ciliopathies, there are unique clinical features. This suggests that while all of the genes associated with these disorders do possess roles in a similar pathway, ciliogenesis and maintenance, they may also play other roles.

Intraflagellar Transport

One of the most well characterized systems in ciliogenesis is the intraflagellar transport pathway. Intraflagellar transport or IFT refers to the complex of proteins which form IFT particles, whose function is to regulate the bi-directional transport of molecules along the ciliary axoneme (Cole et al, 1998). This transport is critical for both the formation and maintenance of cilia. IFT has been shown to be vital for ciliary transport of a wide range of molecules, including tubulins in the formation and maintenance of the ciliary axoneme (Orozco et al, 1999), as well as signaling molecules, such as Gli and smoothened (Huangfu et al, 2003).

IFT is separated into two complexes, depending on whether they regulate retrograde or anterograde ciliary transport. Anterograde transport is carried out by the IFT B complex, which is composed of at least 14 IFT proteins, such as IFT88, 57, and 20 (Rosenbaum & Witman, 2002; Scholey, 2008). The regulated anterograde movement of the IFT B complex and its cargo is carried out through association with the kinesin-2 motor protein (Rosenbaum & Witman, 2002; Scholey, 2008). Retrograde transport is performed by the IFT A complex, which is composed of at least 6 proteins, including IFT140, and 122 (Rosenbaum & Witman, 2002; Scholey, 2008). The motor protein responsible for this regulated movement is dynein (Rosenbaum & Witman, 2002; Scholey, 2008; Sung & Leroux, 2013).

It is not surprising, due to their central importance in ciliogenesis and ciliary maintenance, that defects in IFT transport have been associated with a multitude of ciliopathies (Badano et al, 2006).

Chronic Pancreatitis

Chronic pancreatitis (CP) is a debilitating human condition, characterized by prolonged pancreatic inflammation, and progressive pancreatic degeneration (Brock et al, 2013). This is a relatively rare disorder, affecting between 0.2 and 0.6% of the population in the U.S. and Europe, with an incidence rate of 7-10 per 100,000 (Brock et al, 2013). A major player in the progressive, irreversible nature of CP is pancreatic stellate cell mediated fibrogenesis (Kloppel et al, 2004). This fibrogenesis is initiated by damage to any one or combination of interstitial mesenchymal cells, duct cells, or acinar cells (Schneider et al, 2007). The most commonly injured cells are acinar cells, as these cells are injured through alcohol consumption, the primary cause of chronic pancreatitis (Warren & Murray, 2013). Alcohol consumption results in injury to pancreatic acinar cells, via Vamp8-mediated shift from apical to basal zymogen secretion (Cosen-Binker et al, 2008; Cosen–Binker et al, 2007). Other environmental factors linked to CP are nicotine consumption (Cavallini et al, 1994), and nutritional factors (Grendell, 1983; Levy et al, 1995; Uscanga et al, 1985). Hereditary factors have also been linked to a growing number of cases (Schneider et al, 2002).

The most prominent symptoms presented by patients with CP are severe abdominal pain and steatorrhea, or fatty stools, resulting from malabsorption of dietary fats (Olesen et al, 2013). The severe pain in these patients is often associated with self-medicating behavior, such as malnutrition, nicotine and narcotic consumption (Gardner et al, 2010). Treatment of this disease

is currently limited to pain management (Andren-Sandberg et al, 2002; Warshaw et al, 1998), and dietary changes (Levy et al, 1995). These factors alone stress the need for more substantial treatment options in patients with CP.

While CP, alone, is a serious condition, it is made far worse by the strong link between it and the development of pancreatic cancer. Meta-analysis data shows CP patients as having a relative risk factor of 13.3 for developing pancreatic cancer (Raimondi et al, 2010). Chronic pancreatitis can result in precancerous lesions, such as pancreatic intraepithelial neoplasia, intraductal papillary mucinous neoplasms, and mucinous cystic neoplasms. These lesions can progress into development of pancreatic ductal adenocarcinoma (Yonezawa et al, 2008).

Pancreatic Degeneration in Ciliopathies

One unique ciliopathy phenotype, which is shown in a select number of patients with Oral-Facial-Digital syndrome (OFD) (Chetty-John et al, 2010), von-Hippel-Lindau disease (van Asselt et al, 2013), PKD (Waters & Beales, 2011), and nephronophthisis (Waters & Beales, 2011), is exocrine pancreatic degeneration. This phenotype is less studied in these diseases, and it is likely that upon further inspection, exocrine pancreatic defects may be more common in human ciliopathies than originally thought. The pancreas is organized into two major systems. These are the endocrine and exocrine pancreas. The endocrine pancreas is composed of the islets of Langerhans containing alpha, beta, and gamma cells, which produce and secrete glucagon, insulin, and somatostatin, respectively, to aid in proper glucose metabolism. The exocrine pancreas is composed mainly of acinar cells, which produce and secrete digestive enzymes in the form of non-active zymogens. These zymogens are packed into dense zymogen granules (ZGs), and trafficked to the apical cell surface where ZG contents are released into the acinar lumen in

response to stimuli. Digestive enzymes are then transported through the pancreatic ductal network, and into the duodenum, where they are activated to aid in proper digestion (Bardeesy & DePinho, 2002). It is of interest to note that all cells of the pancreas have primary cilia, except for acinar cells (Aughsteen, 2001; Cano et al, 2006; Nielsen et al, 2008; Zhang et al, 2004).

Pancreatic exocrine degeneration in ciliopathy mouse models is characterized by rapid degeneration of acinar cells at early postnatal stages, alongside of hyperplasia of pancreatic ducts. This phenotype has been characterized in the Orpk, IFT88 hypomorphic mutant mouse model (Cano et al, 2004; Cano et al, 2006; Cervantes et al, 2010; Zhang et al, 2004), as well as in mice with pancreas-specific ablation of Kif3a (Cano et al, 2006). Both of these gene products play roles in anterograde ciliary trafficking. IFT88 is a member of the Intraflagellar Transport (IFT) B complex, and Kif3a is a component of the major anterograde ciliary kinesin motor complex. In both of these models, there is rapid, and robust exocrine pancreatic degeneration, beginning shortly after birth, and pancreatic ductal hyperplasia, occurring either at the same time in Orpk pancreata, or shortly prior at embryonic day 18.5 in Kif3a mutant pancreata. There is near complete loss of primary cilia in all pancreatic compartments of the Kif3a mouse, and a reduction in number and length of primary cilia in the Orpk mouse. Due to the fact that the most deleteriously affected cells in the pancreas, the acinar cells, are the only pancreatic cells that do not possess primary cilia, it has been hypothesized that this degeneration is non-cell autonomous. Specifically, it is believed that ductal cilia play an unknown role in sensation of ductal fluid flow, and that loss of cilia may result in increased intraductal pressure, and downstream acinar injury (Cano et al, 2004; Cano et al, 2006; Zhang et al, 2004).

Chibby

Chibby (Cby) was first discovered as a novel negative regulator of canonical Wnt/β-catenin signaling, via its binding to the C-terminal activation domain of β-catenin (Takemaru et al, 2003). Cby is a relatively small, 14.5 kD, protein which contains a coiled-coil domain, and nuclear localization and export signals (Li et al, 2010). Cby's coiled-coil domain is necessary for its homodimerization and interaction with importin-alpha (Mofunanya et al, 2009). Cby's role in Wnt/β-catenin inhibition is two fold. First, Cby is able to compete with the TCF/LEF transcription factors for β-catenin binding, thus blocking transcriptional activation (Takemaru et al, 2003). This complex is then shuttled out of the nucleus via phosphorylation and subsequent 14-3-3 binding (Li et al, 2008).

A whole-body Cby knockout mouse (Cby-/-) was generated in order to further study the physiological role(s) of Cby. Surprisingly, Cby-/- mice exhibit a multitude of phenotypes, which are currently classified as ciliopathies. On the C57BL/6 genetic background, Cby-/- mice display ~30% embryonic lethality. The rest are born and grossly appear normal at birth but fail to thrive and about 80% show early postnatal death before or shortly after weaning. The surviving Cby-/- mice will mostly catch up in size to their wild-type littermates by about 2 months of age. Included in the phenotypes seen in these mice are chronic sinusitis and otitis, as well as reduced fertility, airway defects, and polycystic kidneys. Cby-/- mice exhibit a paucity of motile cilia in the nasal epithelial and lung airway cells, resulting in an inability to clear mucus and enlarged airway, respectively (Love et al, 2010; Voronina et al, 2009). Cby was found to localize at the base of motile cilia in both of these instances. Subsequently, it was also shown that Cby plays similar roles in primary ciliogenesis (Steere et al, 2012), and that Cby-/- mice display polycystic kidneys (Lee et al, in press), a well-known ciliopathy connected to aberrant primary ciliogenesis (Bettencourt-Dias et al, 2011). In primary cilia, Cby localizes to the transition zone between the

basal body and ciliary axoneme, as well as to the mother centriole in cells that have not yet extended primary cilia. This localization pattern has also been shown in motile cilia (Burke et al, Under revision; Steere et al, 2012).

Pancreatic Degeneration in Cby-/- Mice

In this report, we characterize the exocrine pancreatic degenerative phenotype in Cby-/- mice. Cby-/- pancreata display a rapid exocrine pancreatic degeneration, and ductal hyperplasia, which continues to manifest until a majority of exocrine tissue is lost by 2 weeks. Further characterization indicates that primary cilia are reduced in all regions of the Cby-/- pancreas, and that Cby localizes to the base of primary cilia, as has previously been reported in other cell types (Enjolras et al, 2012; Steere et al, 2012) (Lee et al, in press). We show that the acinar cells themselves have inherent defects, leading to a loss of ZG polarity, and inability to secrete these zymogens in response to stimuli. Similarly, the pancreatic acinar cells from Orpk mice also demonstrated mis-polarization of ZGs. We also show that some components of both anterograde and retrograde IFT complexes are present in acinar cells, specifically localizing to the ZG membranes. Strikingly, transmission electron microscopy (TEM) of purified ZGs shows that unlike wild-type ZGs, Cby-/- ZGs are stuck together in dense clusters with a protein-like structure, indicating that Cby may be necessary for proper maturation and secretion of ZGs. Collectively, our findings raise the possibility that the progressive degeneration of pancreatic acinar cells in ciliopathy models is caused by a cell-autonomous mechanism.

Hedgehog Signaling

The hedgehog (Hh) signaling pathway was originally identified in a genetic screen of *Drosophila melanogaster* (Nusslein-Volhard & Wieschaus, 1980*)*. The name of this pathway

originates from the appearance of disorganized, spiny bristles closely resembling the back of a hedgehog, seen on embryos with null hh alleles (Ingham & McMahon, 2001). The Hh signaling pathway possesses two major receptors. These are the negative regulating receptor, Patched (Ptch) (Nakano et al, 1989), and the positive regulator, smoothened (Smo) (Hooper & Scott, 1989). When the Hh pathway is inactive, Ptch constitutively represses signaling through negative regulation of Smo (Hooper & Scott, 1989; Nakano et al, 1989). While the precise mechanism of this negative regulation is unknown, there are a number of possibilities. Studies suggest that Smo can be activated by oxysterols, and that Ptch may either actively transport an inhibitory ligand to Smo, or an activating ligand, such as oxysterols, away from Smo in the absence of Hh ligand binding (Corcoran & Scott, 2006; Dwyer et al, 2007). It has also been found that, upon activation, Smo will cluster at the plasma membrane, and it has, therefore, been speculated that Ptch actively represses the transport of Smo to the plasma membrane in the absence of signaling (Callejo et al, 2008; Denef et al, 2000; Li et al, 2012).

Whatever the mechanism, the critical step in Hh signaling occurs when the transcriptional regulatory Gli proteins are activated downstream of Smo (Hui & Angers, 2011). The mammalian family of Gli proteins contains three members (Gli1,2 and 3), whereas *Drosophila* contains only one (Ci) (Ingham et al, 2011). In *Drosophila*, Hh signaling results in a shift in post-translational processing of Ci from a transcriptional repressor to an activator (Jiang & Hui, 2008). In vertebrates, the mechanism is very similar, however, the additional family members allow further specialization, where Gli2 is the major activator, and Gli3 is the major repressor (Litingtung & Chiang, 2000; Matise et al, 1998). Gli1, on the other hand, is an activator, which is transcribed downstream of signaling, and acts as a positive feedback regulator to amplify the signal (Park et al, 2000).

While Hh signaling in *Drosophila* occurs primarily at the cell surface, vertebrates utilize the primary cilia to further regulate signaling (Goetz & Anderson, 2010). In fact, in most organisms which contain primary cilia, Hh signaling is almost completely sequestered in the primary cilium, and disruption of the cilium results in equal disruption of Hh signaling (Goetz & Anderson, 2010). Upon ligand binding to Ptch, Ptch levels in the primary cilium are reduced (Rohatgi et al, 2007), and Smo accumulates in its absence (Corbit et al, 2005). Subsequently, Gli2/3 will translocate to the tip of the cilium, in complex with the negative regulator, suppressor of fused (Sufu) (Tukachinsky et al, 2010; Zeng et al, 2010). Through unknown mechanisms, it is thought that interaction between Gli-Sufu and activated Smo leads to the dissociation of Gli from Sufu, where it is then allowed to translocate to the nucleus to activate transcription (Humke et al, 2010). There are many other players in ciliary Hh signaling. One of the most notable is protein kinase A (PKA), which acts as a negative regulator at the base of the cilium, presumably by blocking translocation of Gli-Sufu into the cilium via phosphorylation (Tuson et al, 2011).

Hh signaling is known to play crucial roles in development and homeostasis (Briscoe & Therond, 2013). More recently, aberrant Hh signaling has been linked to tumorigenesis in a number of systems (Teglund & Toftgard, 2010). Specifically, constitutive activation of Hh signaling has been linked to medulloblastoma and basal cell carcinoma (Gailani et al, 1996; Slade et al, 2011; Taylor et al, 2002). A number of other cancers, such as pancreatic, colon, gastric, lung, breast and prostate have been associated with aberrant hyper activation of the Hh signaling pathway (Scales & de Sauvage, 2009). For this reason, it is now more important than ever to fully understand the complexities of Hh signaling mechanisms, and how they are specifically regulated in and by the primary cilium.

Chapter 2 A Novel Role for Ciliary Proteins in Zymogen Granule Secretion of Pancreatic Acinar Cells

2.1 Background

Cilia are separated into two distinct subclasses, referred to as primary and motile cilia. Motile cilia are present on specialized cells, such as mammalian airway epithelia, which express a large number of motile cilia per cell to aid in fluid clearance (Philipps, 1981). Motile cilia may also be expressed as flagella, which are specialized for cell motility in mature sperm (Lindemann & Lesich, 2010), as well as unicellular organisms, such as *Chlamydomonas* (Rosenbaum et al, 1969). Primary cilia are present on nearly all vertebrate cells (Gerdes et al, 2009). While primary cilia were thought to be vestigial for many years, a recent abundance of data has found them to possess many vital roles. These include mechano- and chemo-sensation (Nauli et al, 2013), as well as regulating a number of signaling pathways, such as Wnt (Oh & Katsanis, 2012) and Hedgehog (Goetz & Anderson, 2010). Due to the diversity of functions that cilia possess, there is a corresponding diversity of pathologies associated with aberrant ciliary function, and/or mutation of ciliary genes. These pathologies are collectively referred to as ciliopathies (Waters & Beales, 2011).

There are a number of predominant features, which overlap among the different ciliopathies, such as kidney cysts, polydactyly, and neurological defects (Waters & Beales, 2011). These ciliopathies are typically associated with a number of other, less consistent, phenotypes. While not present in all ciliopathies, a number of human ciliopathies, such as PKD (Waters & Beales, 2011), OFD (Chetty-John et al, 2010), are associated with pancreatic pathologies, including pancreatic ductal cysts and exocrine degeneration. This phenotype has been substantially characterized through studies of the Orpk and Kif3a mutant ciliopathy mouse models (Cano et al, 2004; Cano et al, 2006; Zhang et al, 2004). The Orpk mouse possesses a

hypomorphic allele of IFT88, a major component of the anterograde intraflagellar transport complex (Pazour et al, 2000). Kif3a is a major subunit of the anterograde kinesin motor (Rosenbaum & Witman, 2002), which is essential for ciliogenesis. Both of these mouse models display rapid, progressive, pancreatic acinar cell degeneration, as well as ductal hyperplasia (Cano et al, 2004; Cano et al, 2006; Zhang et al, 2004). Pancreatic islets, and corresponding endocrine function, appear normal in pancreata from both of these models (Cano et al, 2004; Cano et al, 2006; Zhang et al, 2004). Interestingly, acinar cells are the only pancreatic cells which do not normally possess primary cilia (Aughsteen, 2001). Therefore, it has been speculated that these cells are degenerating non-cell-autonomously (Cano et al, 2004; Cano et al, 2006; Zhang et al, 2004).

Cby was originally identified as a novel β-catenin binding partner and negative regulator of canonical Wnt signaling (Takemaru et al, 2003). Cby is a relatively small, 14.5 KDa, protein, containing nuclear import and export domains, as well as a C-terminal coiled-coil domain (Mofunanya et al, 2009; Takemaru et al, 2003). In order to further characterize Cby's physiological role, a Cby-/- mouse was generated (Voronina et al, 2009). Surprisingly, it was found that these mice possess a number of phenotypes, which have been associated with ciliopathies, including sinusitis and otitis (Voronina et al, 2009), airway defects (Love et al, 2010), and cystic kidneys (Lee et al, in press). Subsequently, Cby has been shown to play a role in motile (Burke et al, Under revision; Love et al, 2010; Voronina et al, 2009), and primary (Enjolras et al, 2012; Lee et al, in press; Steere et al, 2012) ciliogenesis.

In this study, we report that Cby-/- mice display rapid, progressive exocrine pancreatic degeneration, and ductal hyperplasia. Cby localizes to the base of pancreatic cilia, and Cby-/- mice display defects in cilia number and length. Taken together, we provide evidence that the

phenotype characterized in these mice is similar to the Orpk and Kif3a mutant mice, and pancreatic degeneration in all of these models may, therefore, share a common mechanism. While pancreatic acinar cell degeneration has been speculated to occur non-cell-autonomously, we provide evidence that refutes this. We show that Cby-/- pancreatic acinar cells possess cell autonomous defects in zymogen secretion.

2.2 Materials and methods

Mouse strains

The generation of Cby mutant mice, and *Tg737*^{orpk} (*Orpk*) mice has previously been described (Voronina et al., 2009, Morgan et al., 1998). All mice were handled according to NIH guidelines, and all experimental procedures were approved by the Institutional Animal Care and Use Committee of the Stony Brook University.

Histological analysis

Mice were euthanized by CO_2 asphyxiation in accordance with Stony Brook IACUC procedures. Pancreata were excised and rinsed in 1 x phosphate buffered saline (PBS), pH 7.4. Washed tissue was then fixed in 4% paraformaldehyde (PFA) overnight at 4°C. Fixed tissue was then washed 3 x 1 hour in 1x PBS at 4°C, with gentle rocking. Following the final wash, tissue was submerged in 70% ethanol in deionized water (DW) overnight at 4°C. Ethanol permeated tissue was then dehydrated through a series of ethanol incubations for 1 hour at room temperature, starting with 80% ethanol in DW, up to 100% ethanol. Following dehydration, tissue was prepared for paraffin embedding by a 1 hour incubation in Histo-Clear (National Diagnostics), then a 1 hour incubation in a 1:1 mixture of Histo-Clear and paraffin, in a vacuum oven at 60°C and -20mmHg. Tissue was then permeated with paraffin via overnight incubation in 100% paraffin at 60°C and -20mmHg. The next day, tissues were placed in molds and embedded in hot paraffin. Blocks were placed on a cold plate to aid in uniform solidification.

Paraffin-embedded pancreas blocks were sectioned on a Leica RM2125 microtome at 5um. Sections were baked onto positively charged slides overnight on a heated slide warmer. Paraffin was cleared from slides by 2 x 10 minute incubations in Histo-Clear at room temperature. Sections were then rehydrated

by 2 minute serial incubations in 100% ethanol, down to 50% ethanol in DW, and finally 100% DW. Rehydrated sections were incubated in Hematoxylin (Sigma) for 5 minutes at room temperature, immediately followed by rinsing with DW. Rinsed sections were then incubated in 1x PBS for 2 minutes for "bluing" of hematoxylin stain. Sections were then dehydrated by reversing the rehydration process; starting at 50% ethanol in DW, and ending in 100% ethanol. Following dehydration, sections were incubated in Eosin (Sigma) for 2 minutes at room temperature, and then rinsed with 100% ethanol. Sections were then incubated 2 x 10 minutes in Histo-Clear before mounting on coverslips with Permount. Slides were imaged with a Leica DM6000 microscope.

Plasmids and transfection

Expression constructs for HA-Cby (Li et al, 2008), Flag-Cby (Li et al., 2008), and Flag-IFT20 were previously described. HEK293T cells were maintained in DMEM or DMEM-GM with 10% FBS and 100 U/ml penicillin-streptomycin. Transfections were performed using ExpressFect (Denville Scientific).

Immunofluorescence microscopy

Adult mice were euthanized by CO_2 asphyxiation. Juvenile mice, up to P5, were euthanized via hypothermia and decapitation, in accordance with approved IACUC protocols. Pancreata were excised and washed in 1x PBS. Tissue was then blot dried with Kimwipes. Blot dried tissue was then embedded in molds with Optimal Cutting Temperature (O.C.T.) compound (Tissue-Tek), being careful to avoid formation of bubbles. Embedded tissue was then placed in liquid nitrogen cooled 2-methylbutane (Fisher) for freezing. Frozen tissue blocks were stored at -80°C until ready to section.

The above-mentioned method of tissue embedding refers to the fresh frozen protocol. Alternatively, tissue can be fixed prior to embedding. In this case, excised pancreata were fixed in 4% PFA overnight at 4°C. Following fixation, tissue was washed with 1x PBS 3 x 1 hour at 4°C, with gentle rocking. Washed tissue was then incubated in 30% sucrose in 1x PBS overnight, or until tissue sank to the bottom. Once permeated with sucrose, tissue was blot dried with Kimwipes and embedded in O.C.T. compound, as described above.

Frozen blocks were removed from -80°C and normalized at -20°C in the cryostat chamber for 1+ hour(s). Normalized blocks were sectioned at 5um, and sections were allowed to dry to positively charged slides for 20 minutes. If fresh frozen, slides were fixed in ice-cold methanol for 5 minutes, followed by washing in 1x PBS 3 x 10 minutes. If tissue was pre-fixed in 4% PFA, proceed immediately to the next step following drying of sections to slides. Slides were then incubated in either 0.1% Triton X-100 (Sigma) or Saponin (Sigma) in 1x PBS 2 x 15 minutes to clear O.C.T. compound, as well as permeabilize sections. Sections were then blocked for 1 hour at room temperature in humidity chambers. Blocking buffer consists of 5% normal goat serum, 0.5% bovine serum albumin (BSA), and 0.1% Triton X-100 or Saponin in 1x PBS. Following blocking, sections were incubated with primary antibody, diluted in tissue diluent, overnight at 4°C in humidity chambers. Tissue diluent consists of 0.5% BSA, and 0.1% Triton X-100 or Saponin in 1x PBS. The following day, sections were washed 3 x 10 minutes in either 0.1% Triton X-100 or Saponin in 1x PBS. Washed sections were then incubated in fluorescently labeled secondary antibody diluted to 1:500 in tissue diluent, for 1 hour at room temperature in humidity chambers. If fluorescently labeled lectins were used, they were added with secondary antibodies in previous step at 1:500 in tissue diluent. Following secondary antibody incubation, sections were washed 3 x 10 minutes in 1x PBS at room temperature. Sections were then

incubated with DAPI for 2 minutes, to stain nuclei. Sections were then rinsed with 1x PBS and then mounted on coverslips with Fluoromount-G (SouthernBiotech).

Images were acquired with a Leica epifluorescence microscope DM 6000 with a 100x/1.3NA objective or LSM 510 confocal microscope (Zeiss) with a 63x/1.4 NA or a 100x/1.4 NA objective.

Apoptosis and proliferation

The level of apoptosis was determined by immunohistochemical analysis of cleaved-caspase 3 expression on paraffin pancreas sections, and averaging the number of labeled cells per field. Proliferation in pancreatic tissue was determined by BrdU incorporation. Mice were given an intraperitoneal injection (IP) of 150 mg/kg BrdU (Sigma), and then euthanized 1 hour later, followed by pancreatic tissue extraction. For proliferation immunofluorescence (IF) staining, one set of serial sections from each mouse were washed with PBS, and BrdU antigen retrieval was performed using 2N HCl treatment for 1 hour at 37°C followed by two washes in 0.1M Borate Buffer (pH 8) and two washes in 1xPBS. All sections were blocked for 2 hours at room temperature with 5% goat serum/0.5% BSA/0.1% TritonX-100/PBS solution and stained with rat anti-BrdU antibody (Accurate, 1:300) overnight at 4°C.

Acinar cell preparation and live cell imaging

Adult mice were euthanized via carbon CO_2 asphyxiation. Pancreata were aseptically extracted and placed in 5 ml ice cold Hank's Balanced Salt Solution (HBSS). Samples were then centrifuged at 2,000 rpm for 2 minutes. Supernatant was discarded and replaced by 5 ml ice cold HBSS. This step was repeated twice for washing. Pancreata were then minced to 0.5-1.0 mm cubes in 5 ml fresh HBSS. This suspension was then centrifuged at 2,000 rpm for 2 minutes at

4°C. Supernatant was discarded and replaced with 5 ml fresh HBSS. This was repeated twice to remove any residual blood and debris. After final centrifugation, supernatant was removed and pancreata were digested in 0.2 mg/ml collagenase P (Roche) in HBSS at 37°C for 16 minutes. Following digestion, 5 ml of 5% fetal bovine serum (FBS) in HBSS was added to quench remaining collagenase P. The sample was then centrifuged at 2,000 rpm for 2 minutes at 4°C. The supernatant was removed and replaced with 5 ml fresh 5% FBS in HBSS. This step was repeated twice for washing. All collagenase P-digested pancreatic tissues were filtered twice through 500-μm polypropylene mesh (Spectrum Laboratories) and subsequently passed through a 201-μm mesh (Spectrum Laboratories). The filtrate was resuspended in cold Waymouth's Media (Waymouth MB 752/1 supplemented with 0.1% BSA, 0.2 mg/ml soybean trypsin inhibitor) and plated onto Cell-Tak (BD Biosciences) coated coverglass plates (MatTek Corp) for live cell imaging. Viability was confirmed by Trypan blue exclusion. For imaging, cells were incubated in Waymouth's media with 2 umol/L FM1-43 (Invitrogen) and imaged on an epifluorescent microscope DM 6000. After obtaining stable fluorescent signal, cerulean was added to a final concentration of 1 nM. Immediately upon adding cerulean, imaging was initiated every 1 minute for 60 minutes. Images were captured with FITC and DIC filters.

Zymogen granule and zymogen granule membrane purification

ZGs were isolated as described previously (4) from murine pancreas. The following buffer was used for homogenization: 250 mM sucrose, 5 mM MOPS, pH 7, 0.1 mM $MgSO_4$, and 0.1 mM phenylmethylsulfonyl fluoride (PMSF), supplemented with protease inhibitor cocktail (Sigma). The tissue was then homogenized with a handheld Tissue Tearer, model number 985370 (Biospec Products, Inc.). The homogenate was centrifuged at 500 x g for 5 minutes at 4°C, and the resulting post nuclear supernatant was centrifuged at 2000 x g for 15 minutes at 4°C to

sediment ZGs. The brownish layer of mitochondria on top of the pellet was removed. If processing for electron microscopy, these purified granules were collected. Otherwise, purified granules were resuspended in 8 mL of 50:50homogenization buffer and Percoll^{TM} (GE Healthcare). This suspension was then centrifuged at 25,000 x g at 4°C for 1.5 hours. The dense white band near the bottom of the centrifuge tube were collected with a plastic pipette and resuspended in homogenization buffer. This suspension was then centrifuged at 2,000 x g for 15 minutes, to remove remaining Percoll. This step was repeated twice for washing. Purified ZGs were then incubated with lysis buffer consisting of: 150 mM sodium acetate, 10 mM MOPS, pH 7, 0.1 mM MgSO4, 27 ug/mL nigericin (Sigma), and 0.1 mM PMSF, supplemented with protease inhibitor cocktail. This mixture is incubated at 37°C for 15 minutes, followed by centrifugation at 100,000 x g and 4°C for 1 hour. The supernatant was saved as ZG content. The ZG membrane pellet was then resuspended in wash buffer consisting of: 300 mM sucrose, 20 mM MES, pH 5.5, 1 mM EGTA, 0.1 mM MgSO4, and 0.1 mM PMSF, supplemented with protease inhibitor cocktail, and centrifuged at 100,000 x g for 1 hour at 4°C to wash residual ZG content. ZG membranes are lysed in 300 mM Tris, 2% SDS, 15% glycerol, and 2% β-mercaptoethanol. This lysate was then processed for SDS-PAGE electrophoresis and western blotting.

Immunohistochemistry

IHC was performed on a Ventana XT (Tucson) autostainer. All IHC was counterstained with hematoxylin. Quantitation represents the average of 15–20 20× fields of view from three mice of each genotype

Transmission electron microscopy

Adult mice were euthanized via CO_2 asphyxiation and their pancreata were extracted. Pancreata were immediately washed in ice cold 1x PBS before submerging in homogenization buffer: 250 mM Sucrose, 5m M MOPS, pH 7.0, 0.1 mM MgSO4, and 0.1 mM PMSF, supplemented with protease inhibitor cocktail (Sigma). The tissue was then homogenized with a handheld Tissue Tearer, model number 985370 (Biospec Products, Inc.). The homogenate was centrifuged at 500 x g for 5 minutes at 4°C, and the resulting post-nuclear supernatant was centrifuged at 2000 x g for 15 minutes at 4°C to sediment ZGs. The brownish mitochondrial pellet on top was removed by gentle pipetting, followed by washing twice with homogenization buffer. The semi-pure white ZG fraction was then suspended in 2% glutaraldehyde and 2% PFA in 1x PBS at pH 7.4. ZGs were incubated in this fixative overnight at 4°C. Samples were then washed in 1x PBS followed by suspending in 2% osmium tetroxide 4°C before dehydration with graded ethanol suspensions. Dehydrated samples were then embedded in Durcupan resin (Sigma) and 80 nm sections were cut with a Reichert-Jung Ultracut E Ultramicrotome. Sections were then mounted on formvar-coated slot copper grids, followed by counterstaning with uranyl acetate and lead citrate. Once prepared, electron micrographs of these sections were taken with a FEI Tecnai12 BiotwinG2 electron microscope and AMT TR-60 CCD digital camera.

Co-immunoprecipitation and western blotting

Culture media and reagents: DMEM/PS consisted of DMEM (Gibco) supplemented with 100U/mL penicillin and 100ug/mL streptomycin. Complete media consisted of DMEM/PS with the addition of 10% FBS. SDS-gel loading buffer consisted of 4% sodium dodecyl sulfate (SDS), 0.2% bromophenol blue, and 200 mM β-mercaptoethanol in 100 mM Tris-HCl, pH 6.8.

Culture and transfection of HEK293T cells: HEK293T cells were obtained from ATCC and maintained at 37°C with 5% CO_2. Upon reaching ~70% confluence, cells were either split or transfected. Cells were split by simple agitation via pipetting up and down. Plasmid DNA was transfected into cells using Expressfect (Denville) per manufacturers instructions. Cells were transfected overnight. The following day, total media was replaced with fresh complete media and cells were allowed an additional 24 to 48 hours of growth before collection.

Immunoprecipitation: Following transfection, HEK293T cells were washed gently with 1x PBS. After washing, cells were lysed in immunoprecipitation buffer (IPB) consisting of 135 mM NaCl, 2.5 mM MgCl2, 1 mM EGTA, 1% Triton X-100, and 10% glycerol, in 20 mM Tris-HCl, pH 8.0, supplemented with protease inhibitor cocktail (Roche). Cells were lysed at room temperature with mild agitation for 20 minutes. Following lysis, samples were collected and centrifuged at 12,000 rpm for 30 minutes at 4°C. Supernatant was collected and incubated with 2 ug anti-Flag antibody (Sigma) overnight at 4°C. The following day, 24 ul of a 1:1 mixture of Protein A and G Sepharose beads (Sigma) was added to the lysates, and they were incubated for

2 hours at 4°C with gently rocking. Samples were then centrifuged at 2,800 rpm for 3 minutes. Supernatant was carefully pipetted off and discarded. 800 ul of IPB was added to the beads. The IPB added in this step may have had modification of NaCl concentration within the range of 135-200 mM in an effort to optimize the ratio of specific to non-specific binding. Samples were then centrifuged at 2,800 rpm for 3 minutes, and supernatant was carefully discarded. This step was repeated an additional 2 times to wash the beads. After washing, 10 ul of IPB was added to beads, along with 10 ul of SDS gel loading buffer. After ensuring that the beads were fully suspended by gently tapping on the tubes, samples were boiled at 95°C to separate bound protein from beads, as well as to denature the proteins. These samples were then stored at -20°C until ready to use.

Western blotting: Lysates were loaded onto SDS-PAGE. Polyacrylamide gels were prepared at 12% for proteins under 80 kDa, or 8% for proteins larger than 80 kDa. After separating proteins adequately by electrophoresis, samples were transferred to nitrocellulose membranes (Bio-Rad) at 220-volt hours. Following transfer, membranes were blocked for 1 hour at room temperature in blocking buffer consisting of 5% fat-free milk and 0.1% Tween-20 in Tris-buffered saline (TBS), pH 8.0. After blocking, membranes were incubated for 1 hour at room temperature in blocking buffer containing primary antibodies. After primary antibody incubation, membranes were washed 3 x 10 minutes in 0.1% Tween-20 in TBS (TBST). Membranes were then incubated in blocking buffer containing horse radish peroxidase-conjugated secondary antibodies for 1 hour at room temperature. Secondary antibody incubation was following by washing 3 x 10 minutes in TBST. Bound proteins were then visualized by chemiluminescent labeling of membranes with HyGlow (Denville), followed by exposure of membranes to Hyblot Cl film

(Denville) in a dark room. Films were then developed on a Konica Medical Film Processor SRX-101A.

Antibodies

Immunoflourecent microscopy:

Primary antibodies used: amylase (Santa Cruz) 1:200, BrdU (Accurate) 1:250, Cby 8-2 (in-house) 1:100, acetylated-α-tubulin (Sigma) 1:1K, insulin (Millipore) 1:500, E-cadherin (BD trans lab) 1:500, Cby 1418p (in-house) 1:100, IFT88 (Proteintech) 1:200, IFT20 (Gregory Pazour, UMASS-Worcester) 1:200

Secondary antibodies used: Alexa Fluor 488 Goat-Anti-Mouse (H+L) (Invitrogen) 1:500, Alexa Fluor 488 Goat-Anti-Rabbit (H+L) (Invitrogen) 1:500, Alexa Fluor 568 Goat-Anti-Mouse (H+L) (Invitrogen) 1:500, Alexa Fluor 568 Goat-Anti-Rabbit (H+L) (Invitrogen) 1:500

Lectins used: Rhodamine labeled Peanut Agglutinin (PNA) (Vector Labs) 1:500, Fluorescein labeled Dolichos Biflorus Agglutinin (DBA) (Vector Labs) 1:500

Western blotting:

Primary antibodies used: IFT20 (Proteintech) 1:250, IFT140 (Proteintech) 1:250, Rab8a (Proteintech) 1:250, Amylase (Santa Cruz) 1:500

Secondary antibodies used: HRP-Goat-Anti-Rabbit IgG (H+L) ML (Jackson ImmunoResearch) 1:5K

Statistical analysis

Two-tailed Student's t test was used for data analysis. *$p < 0.05$, **$p < 0.01$, ***$p < 0.001$, and ****$p < 0.0001$.

2.3 Results

2.3a Pancreatic phenotype of Cby-/- mice

Gross morphology and histology

Cby -/- mice were previously described as possessing ciliopathies (Love et al, 2010; Voronina et al, 2009). While rapid exocrine pancreatic degeneration has previously been described as a ciliopathy (Cano et al, 2004; Cano et al, 2006; Zhang et al, 2004), this phenotype has not been characterized in Cby-/- mice up to this point. The first step in assessing whether these mice display pancreatic degeneration was to analyze the gross morphology of pancreata in wild-type and Cby-/- littermates of comparable size.

Compared to wild-type pancreata, gross morphology showed a large reduction in size of Cby-/- pancreata (Fig. 1A). Also, Cby-/- pancreata were associated with an abnormal abundance of adipose tissue (Fig. 1A). Histological analysis of adult tissue sections revealed that this adipose tissue had replaced areas where pancreatic acinar cells had been lost (Fig. 1B). This phenomenon is known as lipomatosis, and is known to occur in cases of chronic inflammation and degeneration of the exocrine pancreas (Brock et al, 2013).

In order to assess the progression of this phenotype, pancreata were collected from Cby-/- and wild-type littermates at various ages, and histologically analyzed. *In utero*, there were no differences seen between the pancreata of wild-type and Cby-/- mice (data not shown). Knockout pups were able to suckle as digested milk was present in the stomach and fecal pellets were present in the colon. However, histological assessment identified striking lesions in the exocrine pancreas. At birth (P0), while acinar cells appeared normal, there was a slight increase in ductal tissue in Cby-/- pancreata (Fig. 1C,D).

Acinar cell degeneration began to appear at P2-3, and was quite obvious by P7, where, compared to wild-type littermates, Cby-/- pancreata displayed a marked reduction in pancreatic acinar tissue, accompanying the presence of dilated pancreatic ducts (Fig. 1E,F). By two weeks of age ductal and acinar defects were markedly pronounced (Fig. 1G,H). Pancreatic abnormalities of the surviving adult Cby -/- mice also included ductal dilation and loss of a majority of acinar tissue, as well as lipomatosis and fibrosis (Fig. 31,I,J).

Figure 1: Progressive degeneration of Cby-/- pancreata

Pancreata were excised from adult wild-type and Cby-/- mice and photographed for visualization of gross morphology (A). Circled area is pancreatic tissue, while the remaining is adipose tissue, representative of lipomatosis (A). Pancreata from wild-type and Cby-/- mice were analyzed histologically via H&E at various ages (C-J). Arrows point to areas of ductal dilation in Cby-/- pancreata (F,H,J). Low magnification of panel J, to show a larger area of degeneration (B). B-J. Voronina, V and Moon, RT, unpublished data.

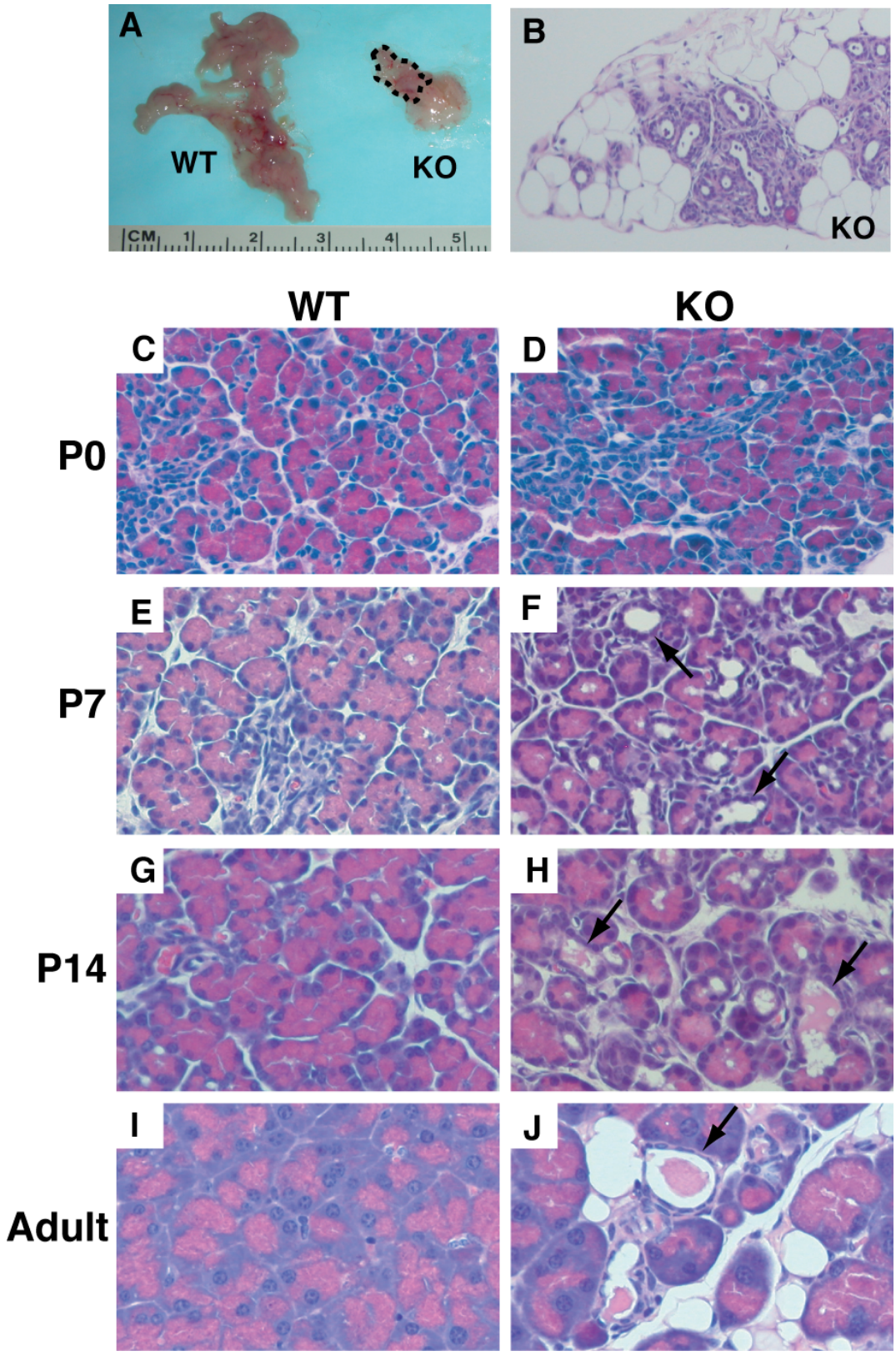

Figure 1: Progressive degeneration of Cby-/- pancreata

Analysis of pancreatic markers

To better understand the nature and timing of pancreatic lesion formation, we analyzed pancreatic sections of newborn and adult Cby-/- mice using an antibody directed against amylase that marks acinar cells and the lectin Dolichos Biflorus Agglutinin (DBA) that marks ductal cells. Despite the normal histological appearance of P0 knockout pancreas, morphometry of the DBA-stained sections demonstrated 2-fold expansion of duct area relative to total tissue area when compared to the control newborn pancreas (Fig. 2A-C). Ductal expansion increases in severity in the surviving adult Cby mutants with a more than 4-fold increase in duct area relative to control littermates (Fig. 2D-F).

Histological analysis of H&E stained pancreatic sections showed that Cby-/- mice have normal islet architecture and immunohistochemical staining of islets for the endocrine markers, insulin and glucagon, was also normal. In all Cby-/- and control animals we observed a normal core of insulin-producing cells surrounded by glucagon-positive cells. Thus, the effect of loss of Cby on pancreatic function is limited to the exocrine pancreas with ductal dilation and acinar degeneration preceding failure to gain weight, while overall endocrine architecture appears to be unaffected.

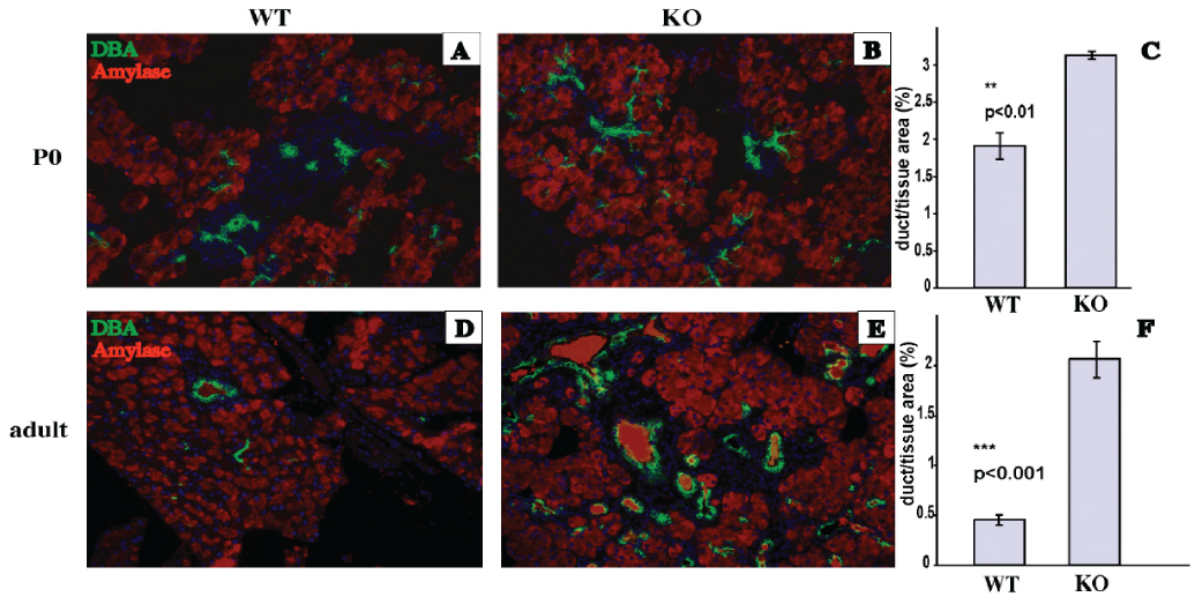

Figure 2: Ductal hyperplasia in Cby-/- pancreata

A-B, D-E. Pancreatic sections of newborn (P0) and adult mice were stained for DBA-lectin (ductal cell marker, green) and amylase (acinar cell marker, red). **C, F**. Mean ratios of ductal area to total tissue (ductal + acinar) +/- s.e.m. are shown for P0 (C) and adults mice (F). For each group three individual animals were used for immunofluorescence, five non-overlapping fields per animal were photographed for quantification. **G**. Voronina, V and Moon, RT, unpublished data.

Apoptosis and proliferation in the pancreas of Cby-/- mice

Both proliferation and apoptosis were analyzed in Cby-/- mice, as Zhang et al. and Cano et al. have shown an increase in both of these processes in IFT88 and Kif3a mutant pancreata, respectively(Cano et al, 2006; Zhang et al, 2004). Pancreatic proliferation was assessed in wild-type and Cby-/- pancreata at P5, and adulthood, via BrdU incorporation. While no significant increase in proliferation was seen in Cby-/- pancreata at P5 (Fig. 3A-C), there was a 16-fold increase in proliferation in adult Cby-/- pancreata, as compared with wild-type controls (Fig. 3D-F). It was also determined that there was an increase in Wnt signaling in Cby-/- pancreata, which may explain this significant increase in proliferation.

Apoptosis levels were determined by immunohistochemically labeling pancreatic sections of wild-type and Cby-/- mice for cleaved caspase 3 (CC3). There was a significant increase in CC3-positive cells in pancreatic sections of Cby-/- mice compared with wild-type controls at P5 (Fig. 5G-I), indicating an increase in apoptosis. Decreased hedgehog signaling seen in Cby-/- pancreata may explain the rapid degeneration seen in Cby-/- acinar cells, as hedgehog signaling has been shown to be vital for proper regeneration of pancreatic acinar cells following injury (Cano & Hebrok, 2008; Cervantes et al, 2010; Kayed et al, 2006).

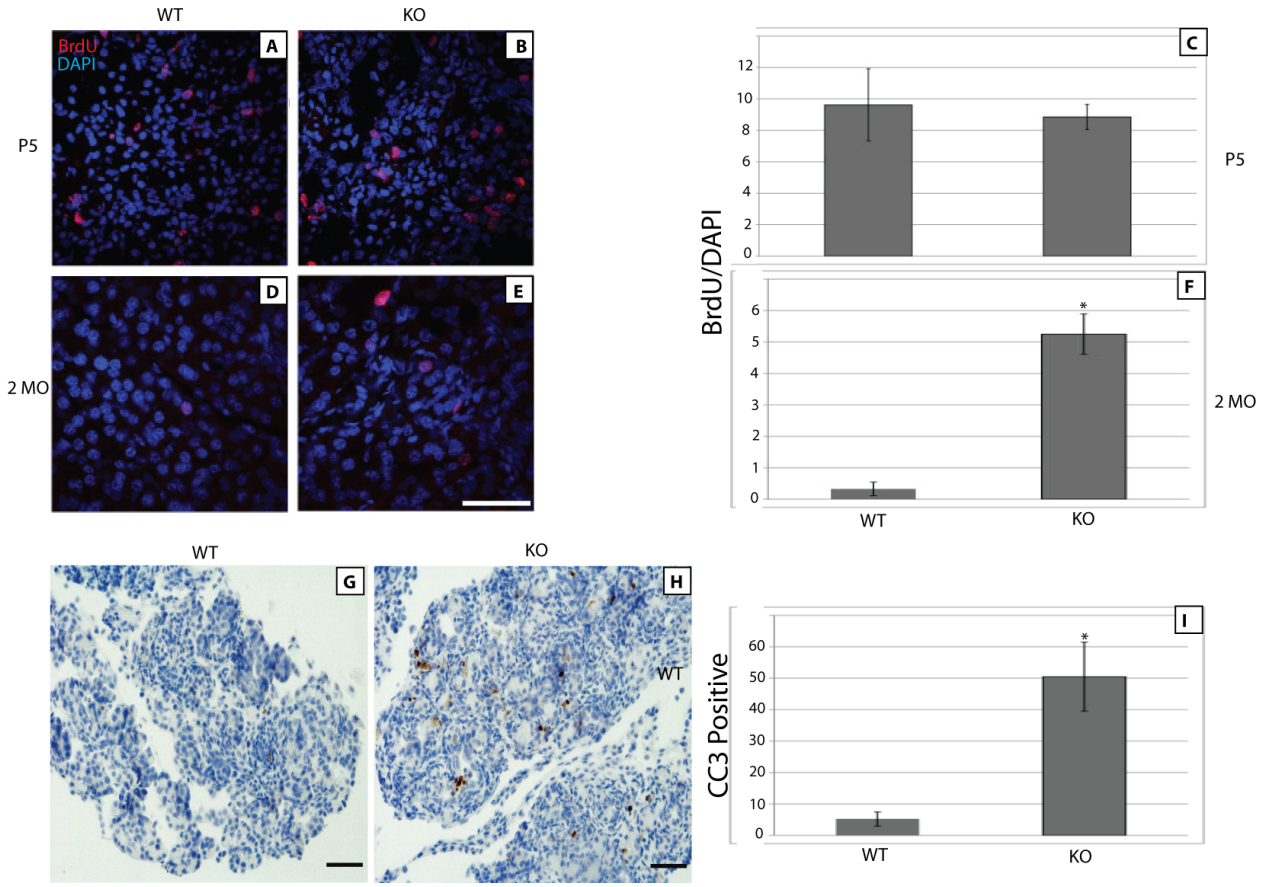

Figure 3: Proliferation and apoptosis in Cby-/- pancreata

Tissue sections labeled with BrdU (red) and DAPI (blue) to analyze levels of proliferation (A-F). Pancreata from P5 display no difference in BrdU labeling (A-B). Quantification of A-B (C). 2-month-old Cby-/- pancreata display a 16-fold increase in BrdU-labeled nuclei (E), compared with wild-type controls (D). Quantification of D-E (F). Scale bar 100 um. P5 pancreata from wild-type and Cby-/- adult mice were labeled with cleaved caspase 3 antibody and hematoxylin to analyze levels of apoptosis (G-H). Scale bars 100 um. Quantification of G-H (I). Quantitation represents the average of 15–20 20 × fields of view from three mice of each genotype G-I. Hall, J. and Crawford, H.C., unpublished data.

Fibrosis and inflammation in Cby-/- pancreata

While characterization of this phenotype has sufficiently defined the pathology displayed in Cby-/- pancreata as pancreatic degeneration, it has not been determined whether this disorder can be classified as chronic pancreatitis. To test this, pancreatic tissue sections were subjected to experiments to determine whether Cby-/- pancreata displayed any hallmark signs of chronic inflammation.

A true marker for chronic pancreatitis is fibrosis of pancreatic tissue, or fibrogenesis (Braganza et al, 2011). In order to determine whether pancreatic tissue was undergoing fibrosis, we stained pancreatic tissue sections from Cby-/- and wild-type controls with trichrome C, a tissue staining agent, which specifically labels collagen deposition, a marker for tissue fibrosis. Indeed, trichrome staining revealed significant accumulation of deposited collagen in Cby-/- pancreata, compared with controls, indicating fibrosis of Cby-/- pancreata (Fig. 4A, B).

In addition to testing for fibrosis, we analyzed Cby-/- pancreata for signs of chronic inflammatory cells. Specifically, we immunohistochemically labeled Cby-/- and wild-type pancreatic tissue sections with markers for leukocytes and mature macrophages. Compared with wild-type controls, Cby-/- pancreata displayed an increase in CD45-labeled leukocytes (Fig. 4C, D), and F4/80-labeled mature macrophages (Fig. 4E,F).

This collection of data allows for classification of the pathology expressed in Cby-/- pancreata as chronic pancreatitis. Since chronic pancreatitis more closely resembles a human pathology than pancreatic degeneration alone, this allows for a more direct translation of this work to human pathology.

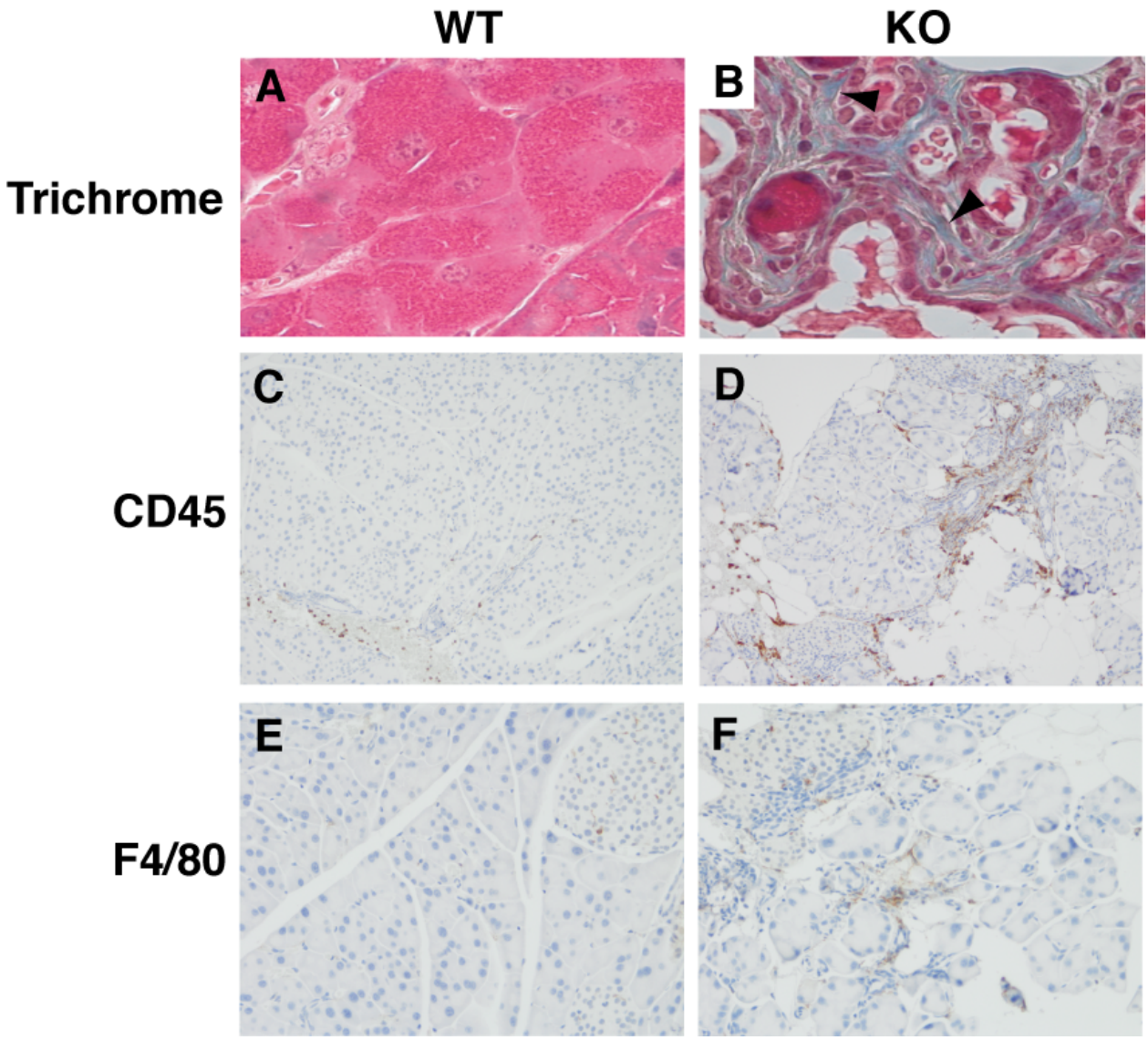

Figure 4: Fibrosis and chronic inflammation in Cby-/- adult pancreata

Adult pancreatic tissue sections were stained with Trichrome C to label collagen deposition (A-B). Arrowheads (B) indicate an increase in collagen deposition in Cby-/- pancreata, compared with wild-type controls (A). CD45 antibody was used to label leukocytes (C-D). Increased CD45 staining is seen in Cby-/- pancreata (D), compared with wild-type controls (C). F4/80 antibody was used to label mature macrophages (E-F). Increased F4/80 staining is seen in Cby-/- pancreata (F), compared with wild-type controls (E). A-B. Voronina, V and Moon, RT, unpublished data. C-F. Hall, J. and Crawford, H.C., unpublished data.

2.3b Pancreatic cilia in Cby-/- mice

Cby localization in pancreatic cilia

Cby was previously reported to be expressed at the base of motile cilia in airway (Love et al, 2010) and nasal epithelial cells (Voronina et al, 2009). More recently, Cby has been shown to localize to the base of primary cilia, as well as at the distal edge of mother centrioles (Lee et al, in press; Steere et al, 2012).

Primary cilia are known to be expressed in pancreatic islet cells, ductal cells, and terminal ductal cells (Rovira et al, 2009). In order to determine whether Cby localization in pancreatic primary cilia resembles the same pattern seen in previous experiments, pancreatic tissue sections from wild-type and Cby-/- mice were fluorescently labeled with antibodies against Cby, and the ciliary marker, acetylated-α-tubulin. In ductal cells which had yet to extend cilia at P15, Cby localized, discretely, to one of two acetylated-α-tubulin-labeled centrioles in all cells (Fig. 5A). Based on knowledge of Cby's localization to mother centrioles (Lee et al, in press; Steere et al, 2012), it is speculated that this pattern is indicative of Cby localizing to mother centrioles in pancreatic ductal cells. Once ductal cells had extended primary cilia, Cby was seen discretely localizing to the base of each cilium (Fig. 5B). This pattern of Cby localization was consistent in primary cilia of terminal ductal cells (Fig. 5C), as well as β-cells in pancreatic islets (Fig. 5D)

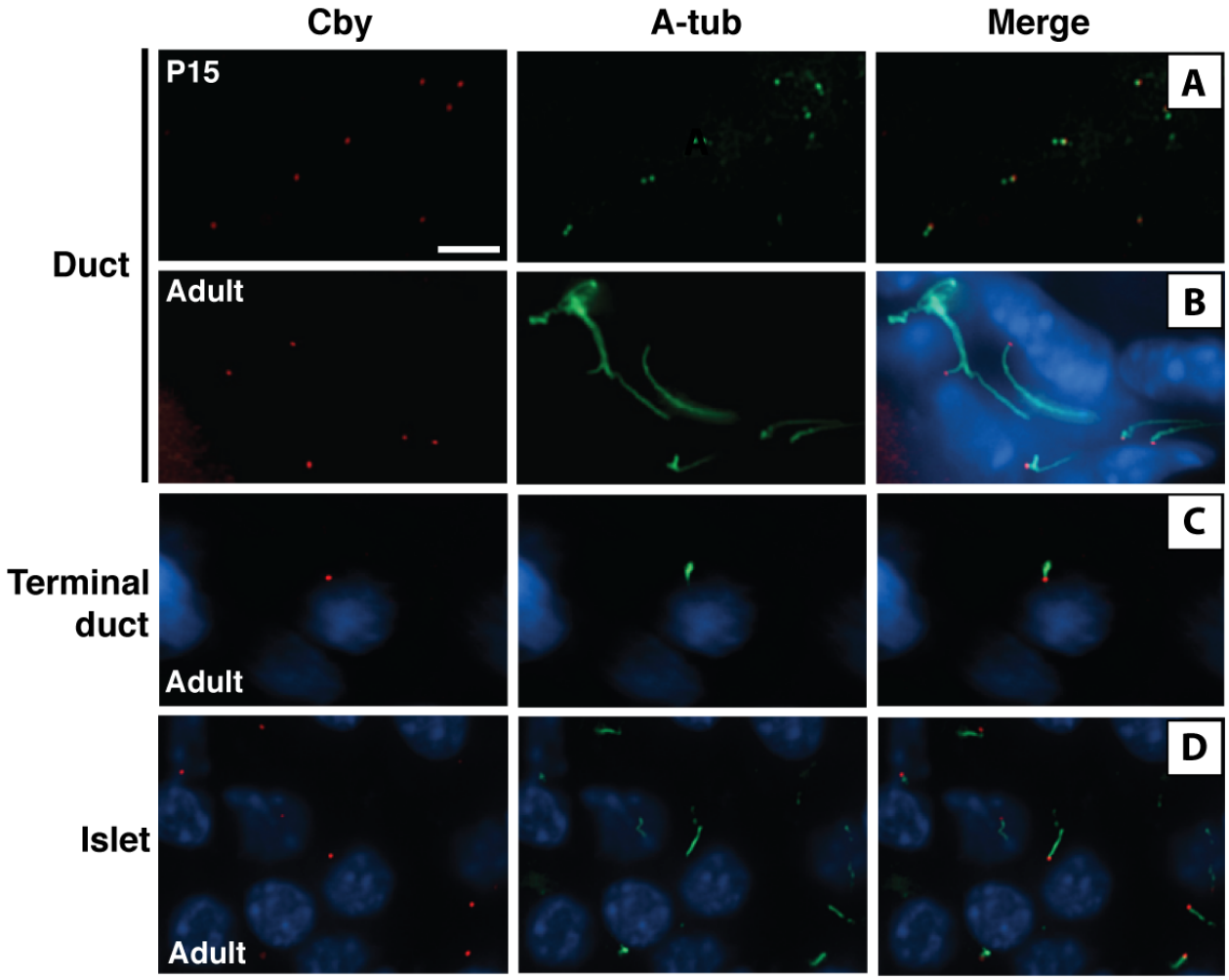

Figure 5: Cby localizes to the base of pancreatic primary cilia

Pancreatic tissue sections were labeled with antibodies against Cby (red) and acetylated-α-tubulin (green). DAPI (blue) labels nuclei. In P15 pancreatic ducts, which have not yet elongated primary cilia, acetylated-α-tubulin labels a pair of centrioles in each cell (A). Cby localizes to one of each of these centrioles (A). Acetylated-α-tubulin labels ciliary axonemes in cells which have elongated primary cilia (B-D). Cby localizes to the base of primary cilia in pancreatic ductal cells (B), terminal ductal cells (C), and pancreatic islet β-cells (D). Scale bar 10 um.

Paucity of cilia in Cby-/- pancreas

Previously, Cby has been shown to regulate cilia formation, and in its absence, examined cells and tissues show a decrease in total number of cilia (Love et al, 2010; Steere et al, 2012; Voronina et al, 2009). As Cby-/- mice display an exocrine pancreatic degeneration phenotype, consistent with models in which there was aberrant expression of ciliary genes IFT88 (Zhang et al, 2004), and Kif3a (Cano et al, 2006), it was hypothesized that Cby-/- pancreata would have a decreased number of primary cilia.

Primary cilia are expressed in pancreatic islet cells, as well as pancreatic ductal cells (Nielsen et al, 2008). In order to assess cilia expression in these compartments, pancreatic tissue sections from Cby-/- and wild-type controls were prepared for immunofluorescent analysis. It was determined that there was a reduction in number and length of acetylated α–tubulin-labeled primary cilia in pancreatic ductal cells of Cby-/- pancreata (Fig. 6B), compared with wild-type controls (Fig. 6A). By co-labeling of sections with acetylated α-tubulin and insulin, was also shown that there was a reduction in number of acetylated α-tubulin-labeled primary cilia in pancreatic islets in Cby-/- pancreata compared with wild-type controls (Fig. 6C,D).

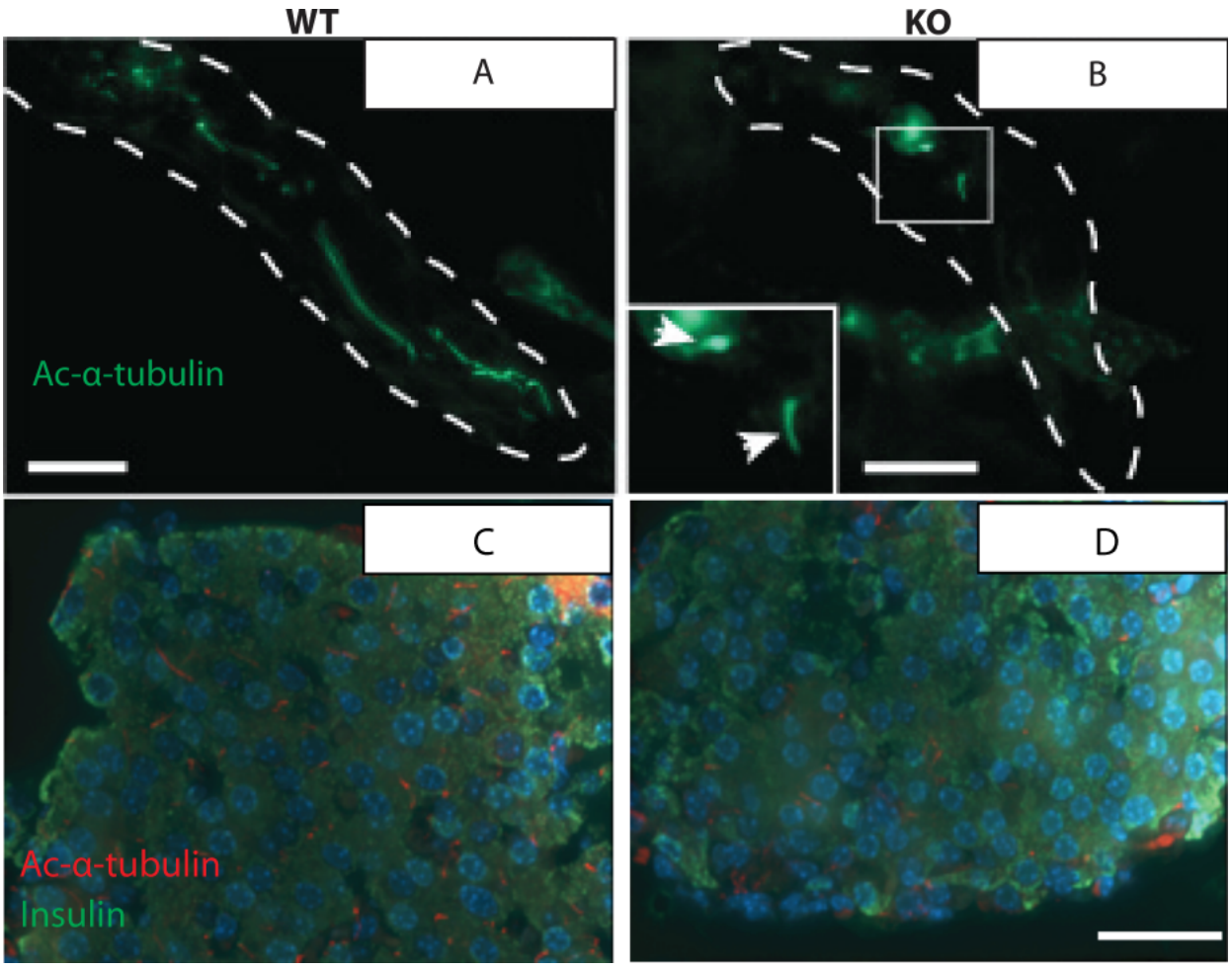

Figure 6: Defect in primary cilia in Cby-/- pancreata

Pancreatic tissue sections were labeled with antibodies against acetylated-α-tubulin to mark for primary cilia (A-B). Scale bar, 10 um. Dotted lines display the outer edge of pancreatic ducts (A-B). Compared with wild-type ducts, which contain elongated primary cilia (A), there is a reduction in both number and length of primary cilia in Cby-/- pancreatic ducts (B). Arrows display shortened cilia in zoomed in panel B. Sections are labeled with antibodies against acetylated-α-tubulin (red) to mark for primary cilia, and insulin (green), as a marker for islets of Langerhans (C-D). Scale bar 50 um. Compared with wild-type controls (C), there is a reduction in number of islet primary cilia in Cby-/- pancreata (D).

2.3c Acinar cell autonomous defects in Cby-/- pancreata

Zymogen granule polarity and secretion defects

In order to determine if there were any autonomous defects in pancreatic acinar cell function, ZGs were fluorescently labeled in wild-type and Cby-/- pancreatic sections with peanut agglutinin (PNA), and E-cadherin. At P0, while acinar cells appeared normal histologically, and had not begun to degenerate, it was seen there was a significant decrease in apically polarized ZGs in Cby-/- acinar cells compared with controls (Fig. 7A-C). At P3, there was a significant shift from apically polarized PNA labeled ZGs in wild-type acinar cells, to basally polarized PNA-labeled ZGs in Cby-/- acinar cells (Fig. 7D-F). To determine whether this change was Cby specific, this same assay was performed on P3 pancreata *Tg737*^{orpk} (*orpk*) mice and wild-type controls, showing a similar pattern of aberrant zymogen granule polarity as Cby-/- acinar cells (Fig. 8A-C). While ZG polarity is disrupted, there was no observed change in acinar cell polarity between Cby-/- and wild-type controls. Taken together, these data indicate a loss of ZG polarity prior to degeneration, and a shift to basally polarized granules at the onset of degeneration in Cby-/- pancreatic acinar cells.

P3 pancreata from wild-type and Cby-/- littermates were also processed for transmission electron microscopy (TEM) in order to assess morphological changes. Not only was ZG polarity shown to be disrupted in Cby-/- acinar cells (Fig. 9C-D), there was a significant increase in total number of ZGs per acinar cell in Cby-/- pancreata, compared to wild-type controls (Fig. 9A-B).

To determine whether these data were indicative of a reduced capacity for zymogen secretion in a cell autonomous fashion, FM1-43 secretion assays (Bombardelli et al, 2010; Cosen-Binker et al, 2008; Cosen–Binker et al, 2007) were performed on isolated acini from Cby-

/- and wild-type control pancreata. As seen in Fig. 10, while there was apically polarized ZG secretion in wild-type pancreatic acinar cells following cerulean stimulation, Cby-/- acini displayed a total absence of stimulated secretion. All of these data together indicated cell autonomous degeneration of pancreatic acinar cells in Cby-/- mice via impaired zymogen secretion.

Figure 7: Aberrant ZG polarity in Cby-/- pancreatic acinar cells

Pancreatic tissue sections were labeled with antibodies against E-cadherin (green), to mark basolateral membranes. Peanut agglutinin (PNA) (red) marks ZG membranes. DAPI (blue) marks nuclei. At P0, wild-type pancreatic acinar cells display apically polarized AG (A). In comparison, Cby-/- ZGs display disrupted polarity (B). Scale bar 10 um. Quantification of ZG polarity in A-B (C). At P3, wild-type pancreatic acinar cells display apically polarized ZGs (D), while ZGs are basally polarized in Cby-/- acinar cells at P3 (E). Apical regions circled by dotted line. Scale bar 10 um. Quantification of D-E (F). Quantitation represents the average of 15–20 20 × fields of view from five mice of each genotype. Number of cells with apical PNA signals divided by the total acinar cell number was used for quantifications. For quantifications, *$P<0.05$.

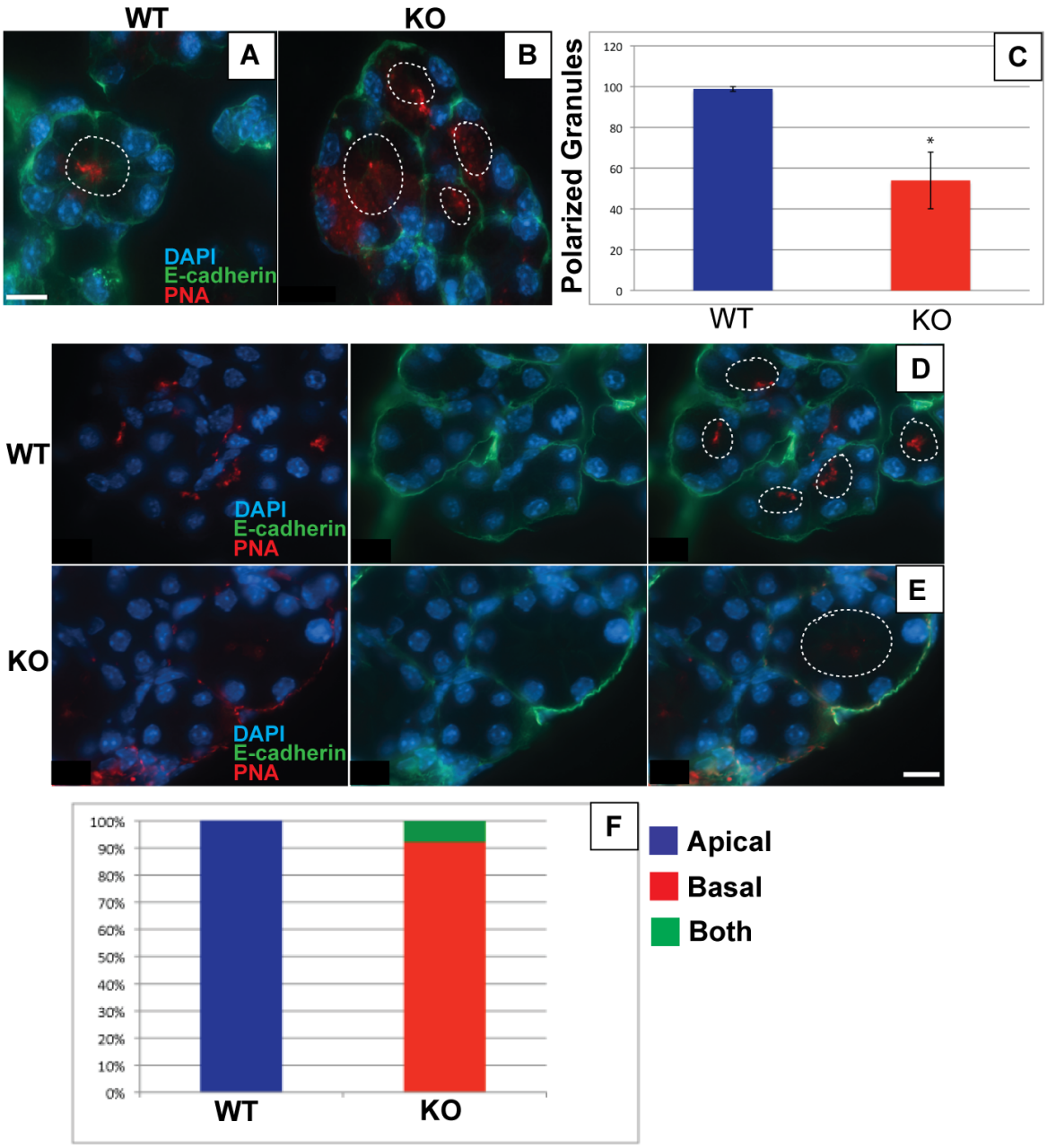

Figure 7: Aberrant zymogen granule polarity in Cby-/- pancreatic acinar cells

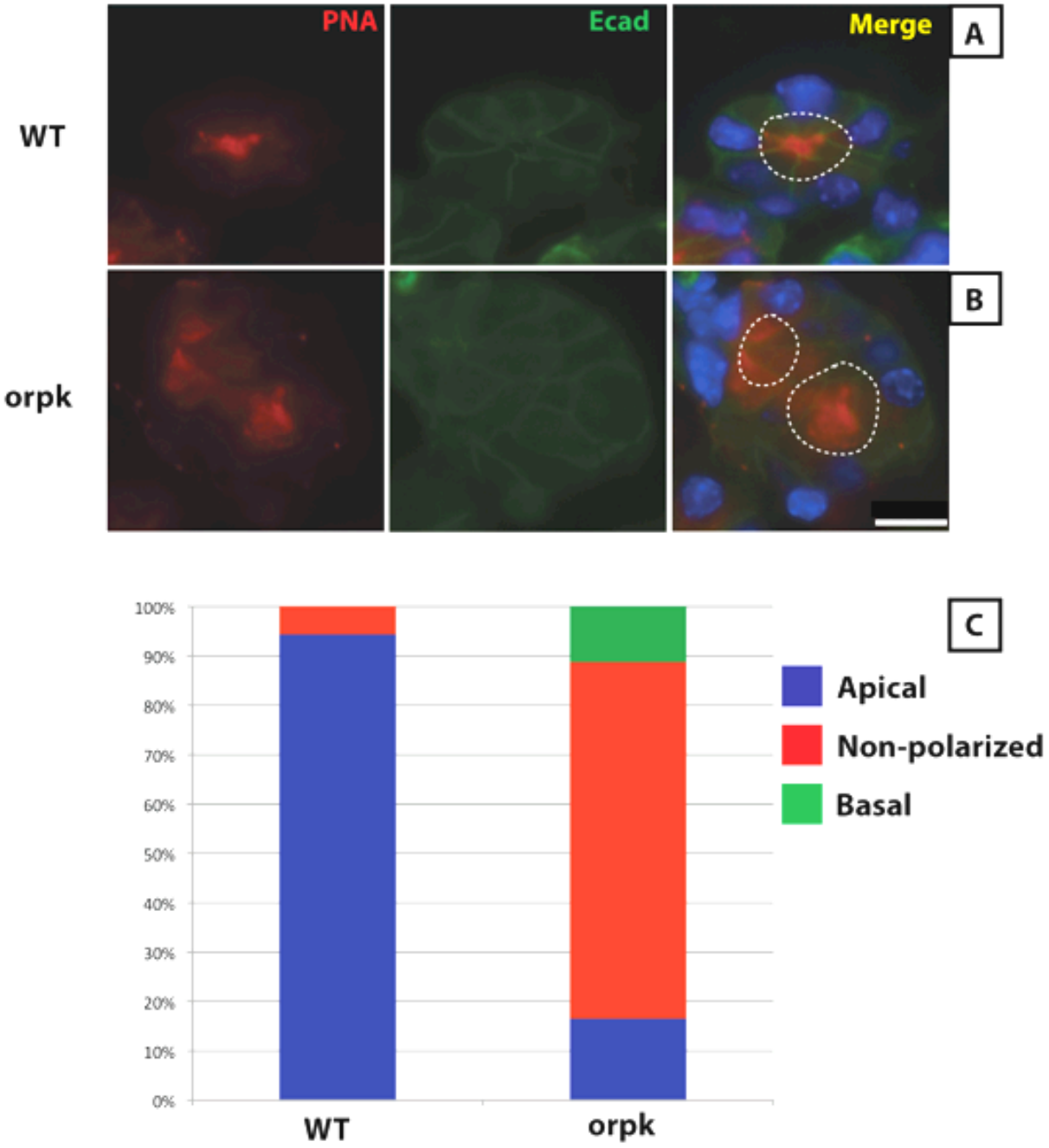

Figure 8: Aberrant ZG polarity in orpk acinar cells

Figure 8: Aberrant ZG polarity in orpk acinar cells

Pancreatic tissue sections of wild-type and orpk P3 mice were labeled with PNA (red), and E-cadherin (green). DAPI (blue) labeled nuclei. Compared with apically polarized ZG in wild-type pancreatic acinar cells (A), orpk pancreatic acinar cells display non-polarized, or basally polarized ZGs (B). Apical regions indicated by dotted line. Quantification of A-B (C). Quantitation represents the average of 15–20 20× fields of view from three mice of each genotype. Number of cells with apical, basal, or non-polarized PNA signals divided by the total acinar cell number was used for quantifications

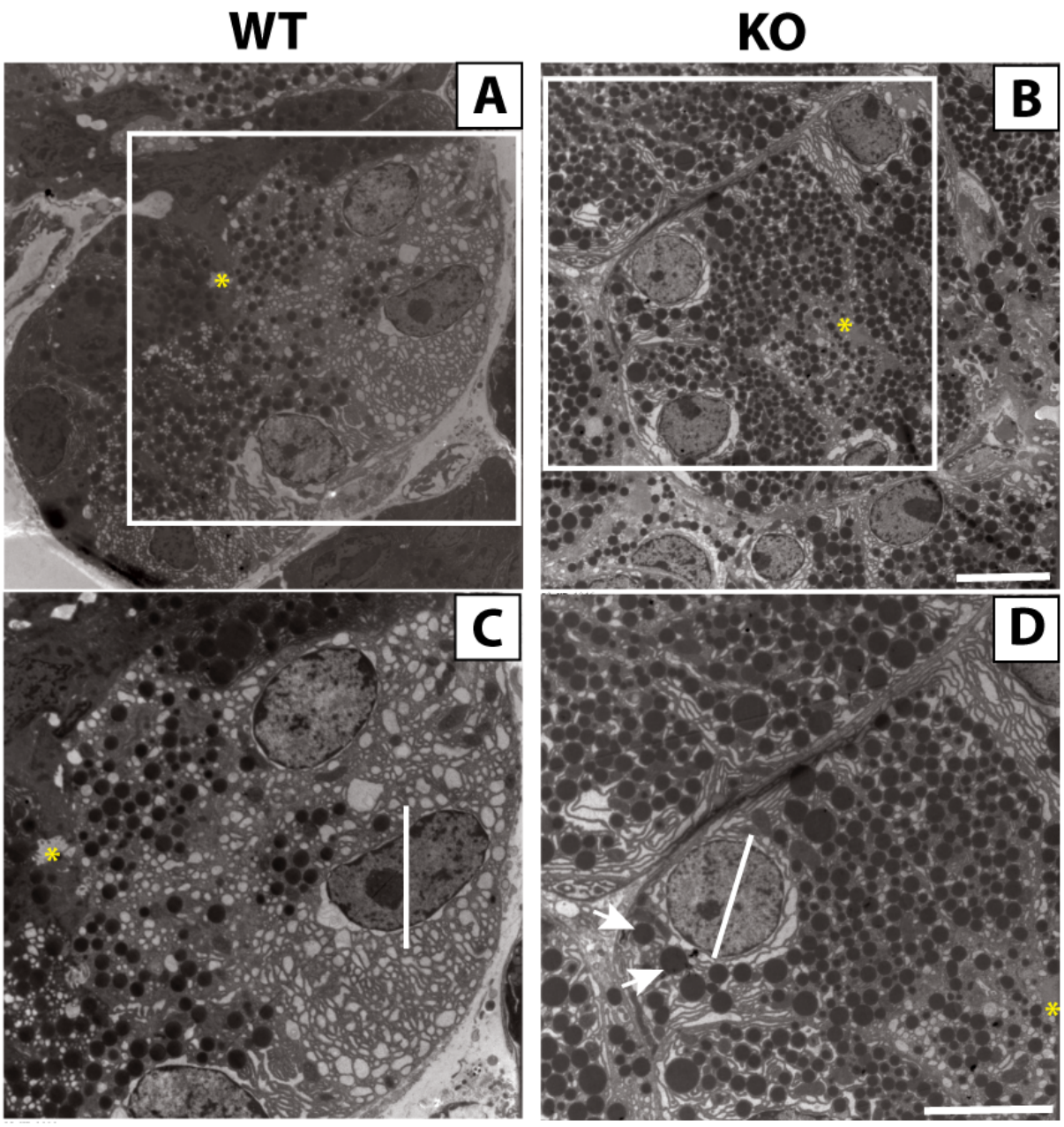

Figure 9: Cby-/- pancreatic acinar cells display increase in ZGs

Figure 9: Cby-/- pancreatic acinar cells display increase in ZGs

P3 pancreata from wild-type and Cby-/- mice were prepared for TEM. Compared with wild-type controls (A), Cby-/- acinar cells display a significant increase in number of ZGs per cell (B). Compared with wild-type controls (C), Cby-/- acinar cells display a significant increase in percent of cells with basal ZGs, indicated with arrows (D). Yellow stars mark apical lumen of acini. Scale bars 10um.

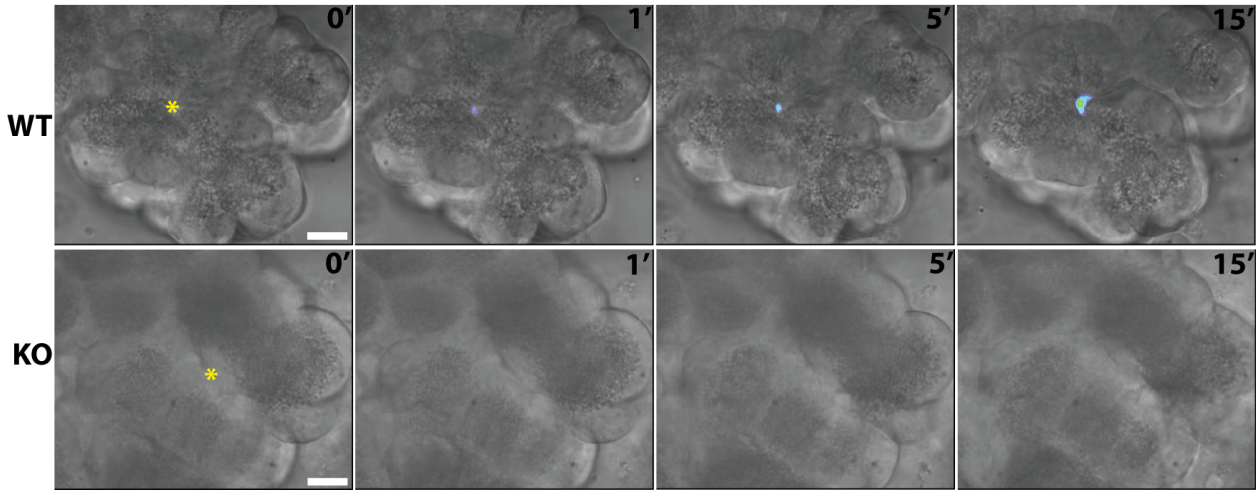

Figure 10: Defective zymogen secretion in isolated Cby-/- pancreatic acinar cells

Isolated pancreatic acinar cells were labeled with FM1-43 membrane binding dye, and prepared for live cell imaging. Following the addition of cearulein, imaging was initiated at time 0'. In wild-type acinar cells, there is gradual, progressive intensity growth of an apical hot spot, indicative of apical zymogen secretion. In comparison, at no point are any hot spots seen in Cby-/- acinar cells. Yellow star indicates apical lumen. Scale bar, 10 um.

Expression and localization of Cby and IFT complex proteins in pancreatic acinar cells

While data indicates an acinar cell autonomous degenerative phenotype in Cby-/-, as well as potentially *Tg737*^{orpk} (*orpk*) mice, expression and localization of Cby and intraflagellar transport molecules in pancreatic acinar cells has not been shown. To determine whether these proteins express, and whether they localize to physiologically relevant subcellular regions within acinar cells, co-immunofluorescence labeling of juvenile pancreatic tissue sections was performed. Antibodies labeling Cby, IFT88, and IFT20 were utilized in conjunction with the ZG membrane binding lectin, PNA. Cby localized to a discrete region at the apical edge of acinar cells, co-localizing with PNA (Fig. 11A). This labeling is absent in Cby-/- acinar cells (Fig. 11B). IFT88 localized in a very similar fashion to Cby, however, in a more diffuse pattern (Fig. 11C). This IFT88 localization pattern was normal in Cby-/- acinar cells (Fig. 11D). IFT20 co-localizes with the medial Golgi marker, HPA, in both wild-type and Cby-/- acinar cells. In addition to this Golgi region, IFT20 co-localized with apical PNA-labeled ZGs in a vesicular pattern (Fig. 11E). While this localization was seen in Cby-/- acinar cells as well, it seemed to co-localize with PNA at a lower level (Fig. 11F).

In order to determine whether these proteins localize to ZG membranes, or associate more transiently, we purified ZGs from wild-type acinar cells via Percoll gradient ultra-centrifugation(Wagner et al, 1994). Following purification, ZGs were separated into content, and membrane fractions via lysis with nigericin buffer. These fractions were separated via SDS-PAGE, followed by western blot analysis. IFT20 was detected in the ZG membrane fraction, while no IFT20 was present in zymogen granule content (Fig. 11G). The retrograde intraflagellar transport complex member, IFT140, also expressed solely at ZG membranes (Fig. 11I),

indicating a potential role for both anterograde and retrograde intraflagellar trafficking complex association with ZG membranes. However, neither Cby, nor IFT88 were detected in ZG membrane or content fractions, raising the possibility that IFT88 association with ZGs might be weak or transient to be detected via this method. While Cby was unable to be detected in these fractions, we were able to show that Cby interacts with IFT20 by co-immunoprecipitation analysis (Fig. 11J), indicating that Cby may be part of a complex at the ZG membrane, however transient.

While crude preparation of ZGs indicated the ability to adequately separate ZGs from the rest of pancreatic tissue, Cby-/- ZGs were unable to be co-purified with wild-type controls via Percoll gradient centrifugation. To assess the cause of this disruption in normal density in Cby-/- acinar cells, crude ZG preparations from Cby-/- and wild-type controls were processed for TEM. Analysis of electron micrographs from wild-type controls showed clean, distinct, and relatively pure ZGs (Fig. 12A,B). In comparison, Cby-/- ZGs formed dense conglomerates, which upon closer inspection, seemed to be due to association with a protein rich structure (Fig. 12C,D).

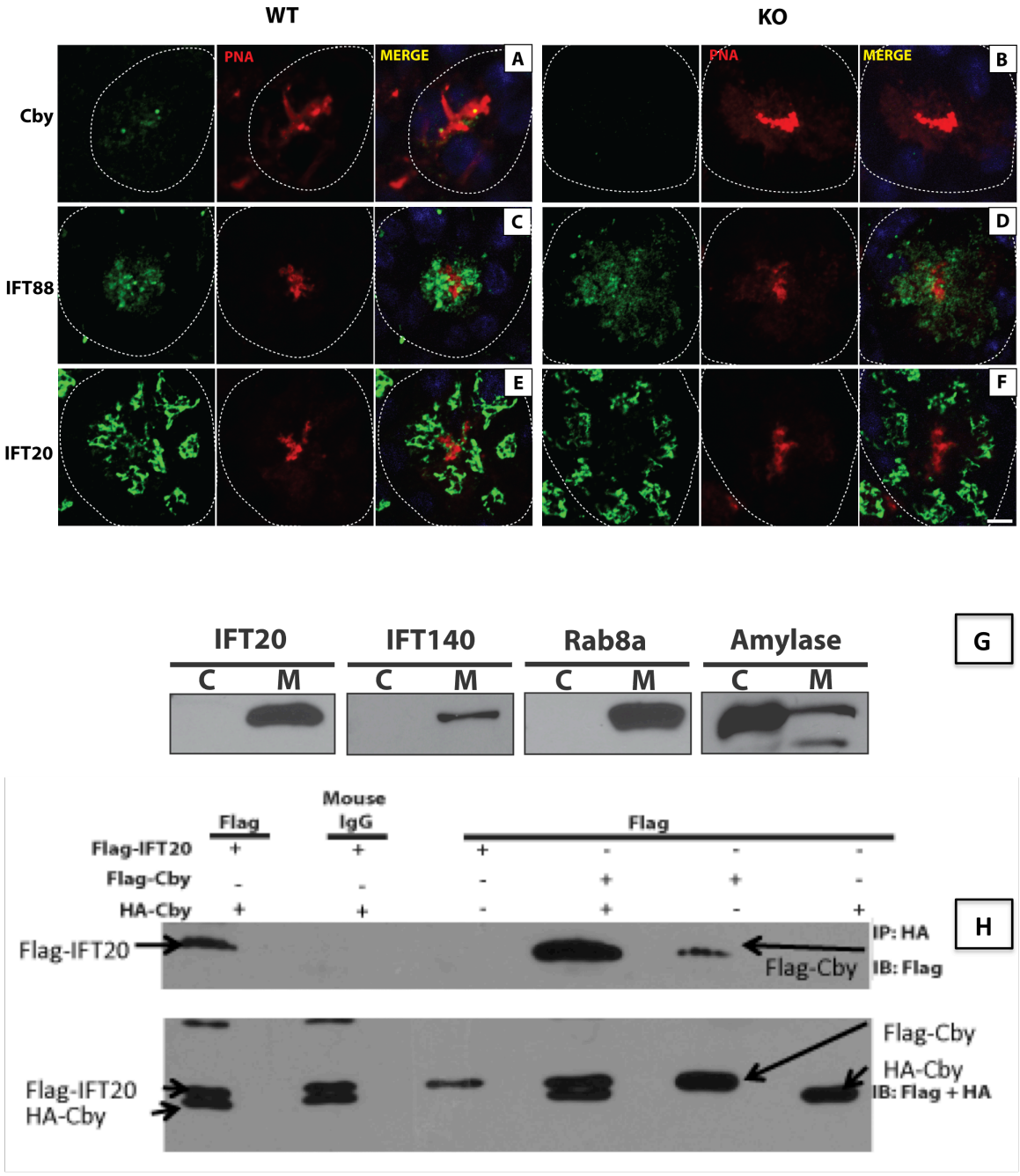

Figure 11: Subcellular localization of Cby and IFT proteins in acinar cells

Figure 11: Subcellular localization of Cby and IFT proteins in acinar cells
P3 pancreatic tissue sections from wild-type and Cby-/- mice were labeled with PNA (red), DAPI (blue), and antibodies against Cby (green) (A-B), IFT88 (green) (C-D), or IFT20 (green). Cby staining in wild-type (A) is specific, as there is an absence of any positive staining in Cby-/- negative controls (B). IFT88 expression and localization pattern is similar in wild-type (C), and Cby-/- (D) acinar cells. IFT20 co-localization with apical PNA is reduced in Cby-/- (F), compared with wild-type (E). Scale bar 10um. ZGs were purified, and then further separated into content C, or membrane M fractions (G). IFT20 and IFT140 are present in the ZG membrane faction (G). Rab8a is a positive control for ZG membranes, and amylase is a positive control for ZG content (G). Co-IP experiment in HEK293T cells transfected with HA-Cby and either Flag-IFT20 or Flag-Cby (H). Both Flag-IFT20 and Flag-Cby are shown to immunoprecipitate with HA-Cby (H).

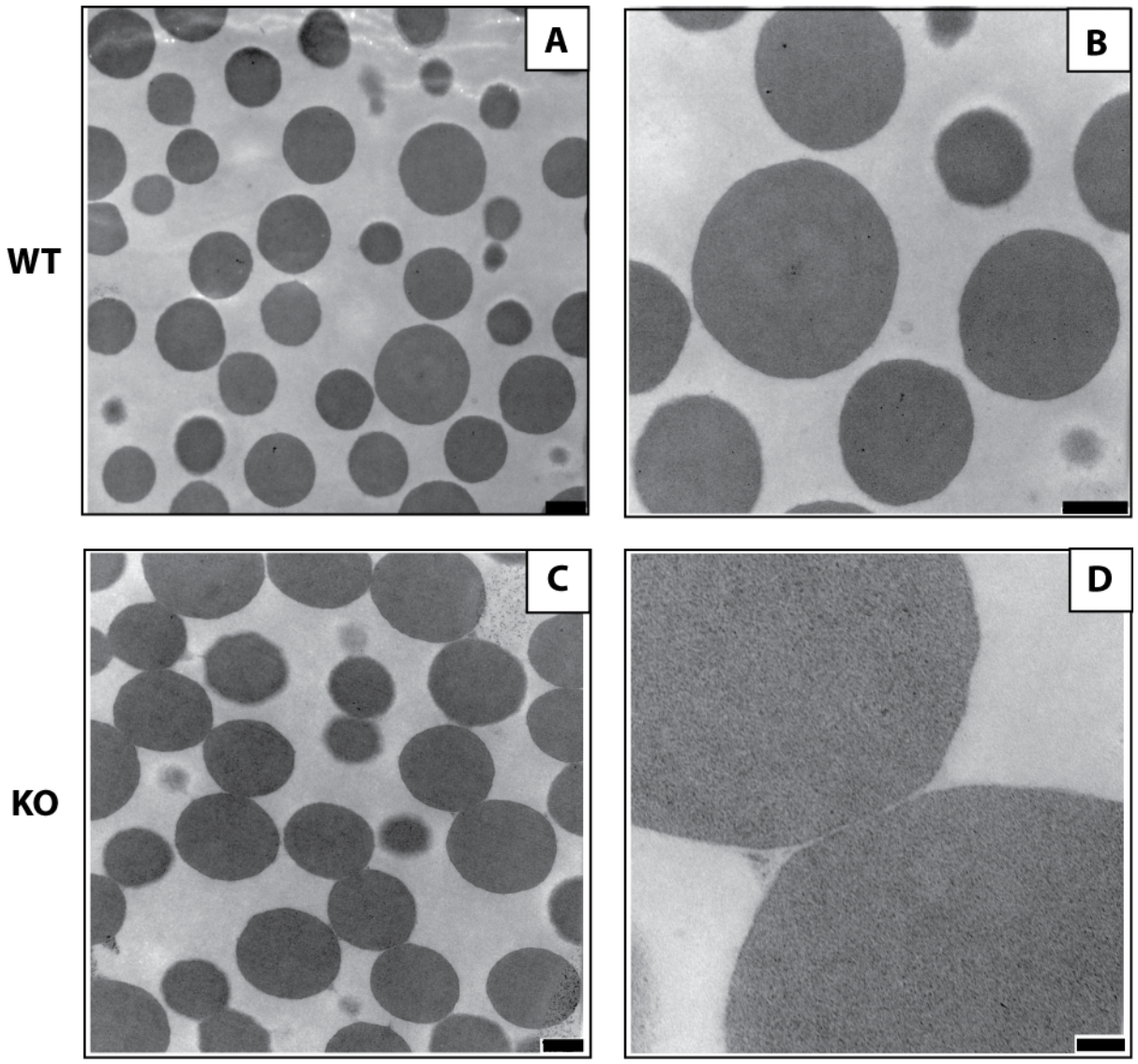

Figure 12: Conglomeration of Cby-/- pancreatic ZGs with electron-dense structure

Purified ZGs from wild-type and Cby-/- mice were subjected to TEM processing. In wild-type, ZGs are shown to be of varying size, and all clean and distinct from one another (A-B). In Cby-/- ZGs are mostly stuck together with an unknown electron dense structure (C-D Scale bars (A-C) 500nm. Scale bar (D) 100nm.

Chapter 3: Cby Plays a Role in Hedgehog Signaling via Regulation of Gli2 Ciliary Trafficking

3.1 Background

The Hh pathway is a major signaling pathway with a multitude of crucial roles in development, and adult homeostasis (Briscoe & Therond, 2013). Defects in this pathway have been implicated in a number of developmental pathologies, as well as cancers (Villavicencio et al, 2000). Recently, strong correlations have been made between ciliary defects and Hh signaling defects (van Reeuwijk et al, 2011). Subsequently, studies revealed a vital regulatory role or primary cilia in Hh signaling (Goetz & Anderson, 2010; Keady et al, 2012; Tukachinsky et al, 2010).

The glioma (Gli) proteins serve as key transcriptional regulatory of mammalian Hh signaling (Hui & Angers, 2011). While Gli1 and 2 act as transcriptional activators, Gli3 is a transcriptional repressor (Hui & Angers, 2011). In the absence of signaling, Gli2 and 3 are separately associated in complexes with Sufu (Haycraft et al, 2005). These complexes are phosphorylated by PKA (Chen et al, 2011), and subsequently bound by 14-3-3, which prevents translocation of these complexes into the ciliary compartment (Asaoka et al, 2009). In the presence of Hh ligand, the negative regulatory receptor, Ptch, translocates out of the ciliary membrane compartment (Rohatgi et al, 2007), while Smo accumulated at the ciliary membrane (Wang et al, 2009). This leads to downregulation of PKA phosphorylation of Gli-Sufu, and subsequent translocation of these complexes to the tip of the cilia (Tukachinsky et al, 2010). Through an unknown mechanism, presumably via association with activated Smo, Gli2 and 3 dissociate from Sufu and translocate out of the ciliary compartment (Tukachinsky et al, 2010). While this results in loss of repressive activity of Gli3, Gli2 is free to enter the nucleus and

activate transcription of Hh target genes (Haycraft et al, 2005). One of these genes is Gli1, which acts downstream of initial pathway activation in a positive feedback loop (Park et al, 2000).

Cby was originally identified as a novel negative regulator of Wnt/β-catenin signaling (Takemaru et al, 2003). Cby binds nuclear β-catenin, thereby inhibiting its transcriptional activity (Takemaru et al, 2003). This complex is dually phosphorylated by Akt and subsequently bound by 14-3-3 (Li et al, 2008). This tri-partite complex is then shuttled out of the nucleus (Li et al, 2010). More recently, Cby was found to play a role in ciliogenesis (Burke et al, Under revision; Lee et al, in press; Love et al, 2010; Steere et al, 2012; Voronina et al, 2009), and to localize to the ciliary transition zone (Burke et al, Under revision; Lee et al, in press; Steere et al, 2012). Due to this localization pattern, and Cby's role in a similar shuttling process with 14-3-3, we hypothesized that Cby may regulate ciliary Gli trafficking.

Here, we show that Cby binds to all three mammalian Gli homologues. Also, in the absence of Cby, there is an accumulation of Gli2 at the tips of primary cilia, indicating that Cby regulates ciliary trafficking of Gli proteins. In addition, we show that Cby may compete with 14-3-3 for Gli2 binding. While further work is warranted, these findings suggest a novel role for Cby in regulation of mammalian Hh signaling.

3.2 Materials and Methods

Plasmids

Expression constructs for HA-Cby (Li et al, 2008), HA-14-3-3 (Li et al., 2008), and Flag-Gli1,2 and 3 were previously described.

Co-immunoprecipitation and western blotting

Co-imunoprecipitation and western blotting were performed as described in the Materials and Methods section in Chapter 2.

Cell lines and cell culture

HEK293T cells were maintained in DMEM or DMEM-GM with 10% FBS and 100 U/ml penicillin-streptomycin. Transfections were performed using ExpressFect (Denville Scientific). RPE1 cells were obtained from ATCC, and mouse embryonic fibroblasts (MEFs) were collected from wild-type and Cby-/- mice as previously described (add references). MEFs were maintained in DMEM with 10% FBS (Denville Scientific) with 100U/ml Penicillin-Streptomycin (Gibco), at 37°C with 5% CO_2. To generate stable Cby knock-down (Cby KD) RPE1 lines, cells were transfected with Sure Silencing™ pGeneClip™ plasmid, containing scrambled sequence (control) or short hairpin RNA for Cby (NM_015373) (GGCTGAAAGTGGACATCTTAT) under U1 promoter control, with a puromycin resistance gene. Expressfect (Denville) was used for transfection according to manufacturer's instructions. After selection with 2.5 ug/ml Puromycin (Gemini BioProducts), transfected cells were maintained in medium supplemented with 1.25 ug/ml Puromycin. Describe how ciliogenesis was induced.

SAG treatment and immunofluorescence microscopy

Cells were either treated with 200 nM SAG (Axxora) or control for 24 hours. Cells were fixed on coverslips in ice-cold methanol for 5 minutes. Following fixation, cells were washed with 1x PBS. Washed cells were blocked for 1 hour in blocking buffer containing 5% normal goat serum, 0.5% BSA, and 0.1% Triton X-100 in 1xPBS. After blocking, cells were incubated with primary antibody overnight at 4°C. The next day, cells were washed 3 x 5 min in 1xPBS. Cells were then incubated for 1 hour at room temperature with fluorescently conjugated secondary antibody. Cells were then washed 3 x 5 minutes in 1xPBS. Following washing, cells were incubated in DAPI for 2 minutes at room temperature. Cells were then rinsed with 1xPBS and mounted on slides with Fluoromount-G (SouthernBiotech).

Images were acquired with a LSM 510 confocal microscope (Zeiss) with a 63x/1.4 NA objective.

Antibodies

Immunofluorescent microscopy:

Primary antibodies used: acetylated-α-tubulin (Sigma) 1:1K, Gli2 (Jonathan Eggenschwiler, University of Georgia) 1:200

Secondary antibodies used: Alexa Fluor 488 Goat-Anti-Rabbit (H+L) (Invitrogen) 1:500, Alexa Fluor 568 Goat-Anti-Mouse (H+L) (Invitrogen) 1:500

Western blotting:

Primary antibodies used: anti-HA (Roche) 1:500, Flag f3165 (Sigma) 1:500

Secondary antibodies used: HRP Anti-Rat IgG (H+L) (Roche) 1:5K, HRP Goat-Anti-Mouse IgG (H+L) ML (Jackson ImmunoResearch) 1:5K

3.2 Results

Cby interacts with Gli transcription factors

Cby is known to localize to the base of cilia (Enjolras et al, 2012; Love et al, 2010; Voronina et al, 2009). Recently, localization of Cby to this region has been further narrowed down to the ciliary transition zone (Burke et al, Under revision; Lee et al, in press). It is widely accepted that the ciliary transition zone may act as a gate for regulated entry and exit from the ciliary compartment. (Williams et al, 2011). Whether Cby itself plays any particular role as a gatekeeper in this region, has yet to be explored.

During Hh pathway activation, there is tightly regulated trafficking, into and out of the cilium, a number of Hh pathway modulators (Nielsen et al, 2008; Rohatgi et al, 2007; Wang et al, 2009). Of these, Gli proteins are known to transiently, and specifically translocate to the tips of primary cilia (Jia et al, 2009; Tukachinsky et al, 2010). To test whether Cby has any direct effect on this process, we first performed Co-IP experiments to determine if Cby interacted with any of the mammalian Gli family members. We found that Cby strongly and specifically interacts with Gli1, 2, and 3 (Fig. 13). Of these interactions, that between Cby and Gli2 was found to be the strongest. Confirmation of these interactions warranted further exploration into the possibility of Cby regulating ciliary Gli trafficking.

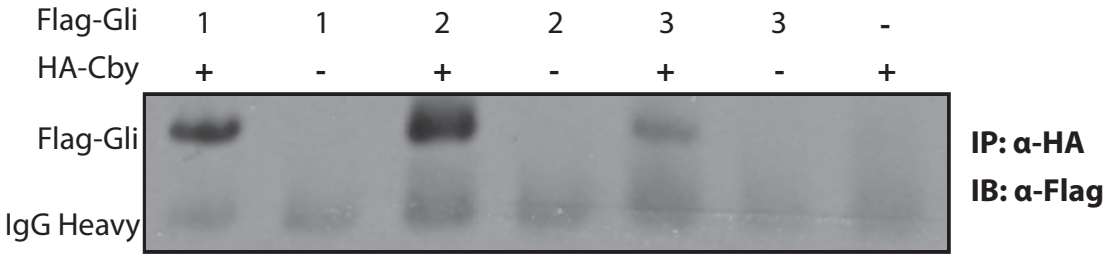

Figure 13: Cby interacts with Gli1, 2 and 3

HEK 293T cells were transfected with plasmids containing Flag-Gli1, 2, or 3, in the presence (+) or absence (-) of HA-Cby. Lysates were then immunoprecipitated with α-HA antibody, followed by blotting with α-Flag antibody. Flag-Gli1, 2, and 3 all specifically pulled down with HA-Cby, with the interaction between HA-Cby and Flag-Gli2 being the strongest, and between HA-Cby and Gli3 being the weakest. Li, F.-Q., unpublished data.

Loss of Cby results in aberrant increase in localization of Gli2 at the tip of cilia

Cby localizes to the ciliary transition zone, and interacts with all three mammalian Gli transcription factors. To determine whether Cby regulated entry or exit of these proteins from the ciliary compartment, we analyzed Gli2 ciliary localization in response to treatment with the Smo agonist, SAG (Tukachinsky et al, 2010). Gli2 was chosen, as out of the 3 family members, Cby was found to interact most strongly with Gli2. Also, Gli2 is the primary positive transcriptional regulator of Hh signaling.

First, this experiment was performed in mouse embryonic fibroblasts (MEFs) from Cby-/- and wild-type control mice. Cells were either treated with SAG or left untreated, and then fixed and collected for analysis of Gli2 ciliary localization. Strikingly, we found that even in the absence of agonist, there was a robust accumulation of Gli2 at the tip of cilia in Cby-/- MEFs (Fig. 14C) compared with wild-type controls (Fig. 14A). This was further manifested in SAG treated Cby-/- MEFs (Fig. 14D), while there was only a mild increase in Gli2 ciliary tip localization in SAG-treated wild-type MEFs (Fig. 14B). These data indicate that Cby plays some role in Gli2 ciliary trafficking.

To determine whether this change in Gli2 ciliary trafficking is dose dependent on Cby expression, or if this is only an all or none event, we performed this same experiment using RPE1 cells in which Cby was knocked down (Cby KD), or treated with a scrambled control. We found that while less dramatic than in MEFs, Cby expression levels affected Gli2 ciliary trafficking. When left untreated, there was no discernable difference in Gli2 ciliary levels between Cby KD (Fig. 15C), and control RPE1 cells (Fig. 15A). However, when treated with

SAG, there was a significant increase in Gli2 ciliary tip accumulation in Cby KD RPE1 cells (Fig. 15D), compared with controls (Fig. 15B).

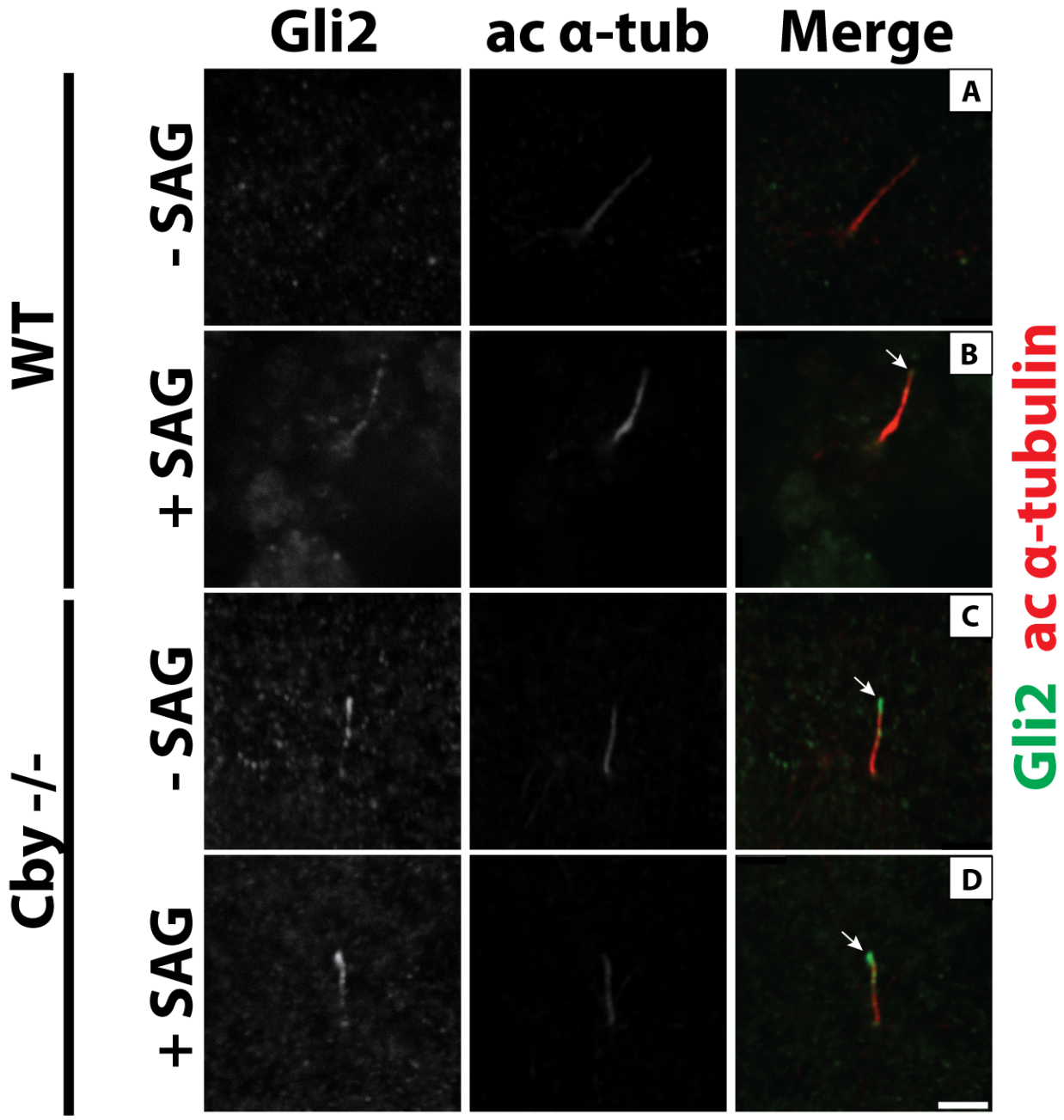

Figure 14: Increase in ciliary tip localization of Gli2 in Cby-/- MEFs

Figure 14: Increase in ciliary tip localization of Gli2 in Cby-/- MEFs

Cby-/- and wild-type control MEFs were either untreated (A,C), or treated with SAG (B,D). Cells were labeled with antibodies against Gli2 (green) and acetylated-α-tubulin (red, to mark cilia. In untreated cells, there is significant increase in ciliary localization of Gli2 between control (A) and Cby-/- cells (C). In the presence of SAG, there is a significant increase in ciliary tip localization of Gli2 in Cby-/- cells, compared with controls. Scale bar, 1 um. Ciliary tip localization of Gli2 is depicted by arrows (B,C,D).

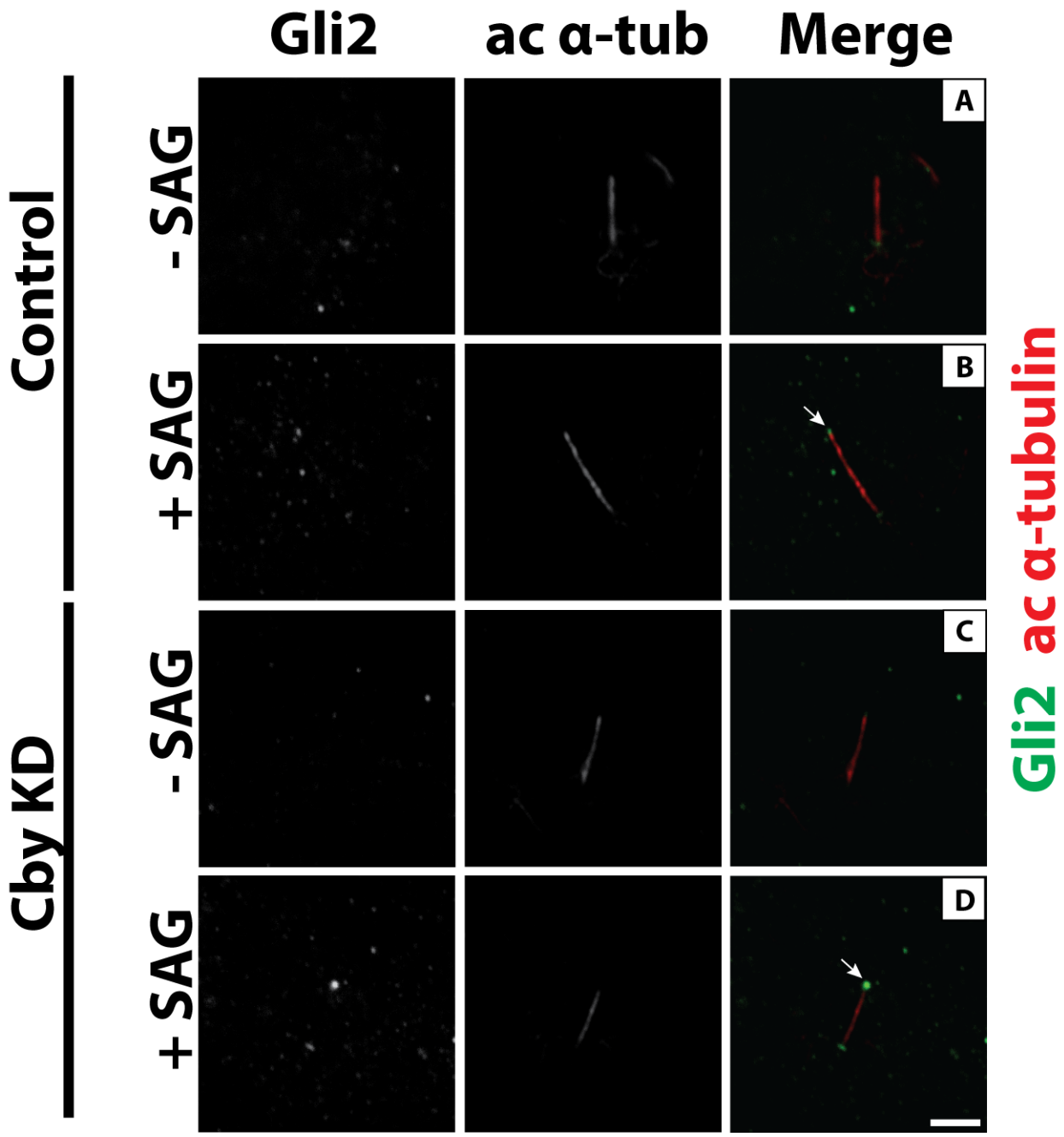

Figure 15: Reduction of Cby results in increased Gli2 ciliary tip localization in RPE1 cells

Figure 15: Reduction of Cby results in increased Gli2 ciliary tip localization in RPE1 cells

Cby KD and control RPE1 cells were either untreated (A,C), or treated with SAG (B,D). Cells were labeled with antibodies against Gli2 (green) and acetylated-α-tubulin (red, to mark cilia. In untreated cells, there is no discernable difference in ciliary localization of Gli2 between control (A) and Cby KD cells (C). In the presence of SAG, there is a significant increase in ciliary tip localization of Gli2 in Cby KD cells, compared with controls. Scale bar 1 um. Ciliary tip localization of Gli2 is depicted by arrows (B,D).

Cby may compete with 14-3-3 for Gli2 binding

Since Cby expression levels, and not just whether or not it is expressed, affect Gli2 ciliary tip accumulation, it is likely that Cby elicits its regulation of this process through direct binding of Gli2, rather than through indirect transcriptional regulation. 14-3-3 has recently been discovered as a negative regulator of Hh signaling though interaction with Gli proteins, and inhibition of their ciliary trafficking (Asaoka et al, 2009). Cby has been found to interact with 14-3-3, in a complex with β-catenin, when aiding in the shuttling of this complex from the nucleus (Li et al, 2010; Li et al, 2008). We hypothesized that Cby may form a complex with Gli2 and 14-3-3, and assist in negative regulation of Gli2 ciliary shuttling.

To test this, we performed a series of Co-IPs in which we pulled down 14-3-3 with Gli2, while altering levels of co-transfected Cby. If Cby formed a complex with these proteins, there would be a proportional increase in 14-3-3-Gli2 binding in the increasing presence of Cby. However, we found the opposite to be true. As Cby levels were increased, there was a decrease in 14-3-3 pulled down by Gli2 (Fig. 16). This data indicates that, since Cby and 14-3-3 are known to interact with Gli2, Cby and 14-3-3 compete for Gli2 binding.

This piece of evidence introduced the possibility that, rather than negatively regulating, Cby may be positively regulating Hh signaling though regulation of Gli2 ciliary trafficking. It is possible, therefore, that Cby may aid in the exit of Gli2 from the cilia, rather than inhibit its entrance. This, and other possibilities still need to be tested.

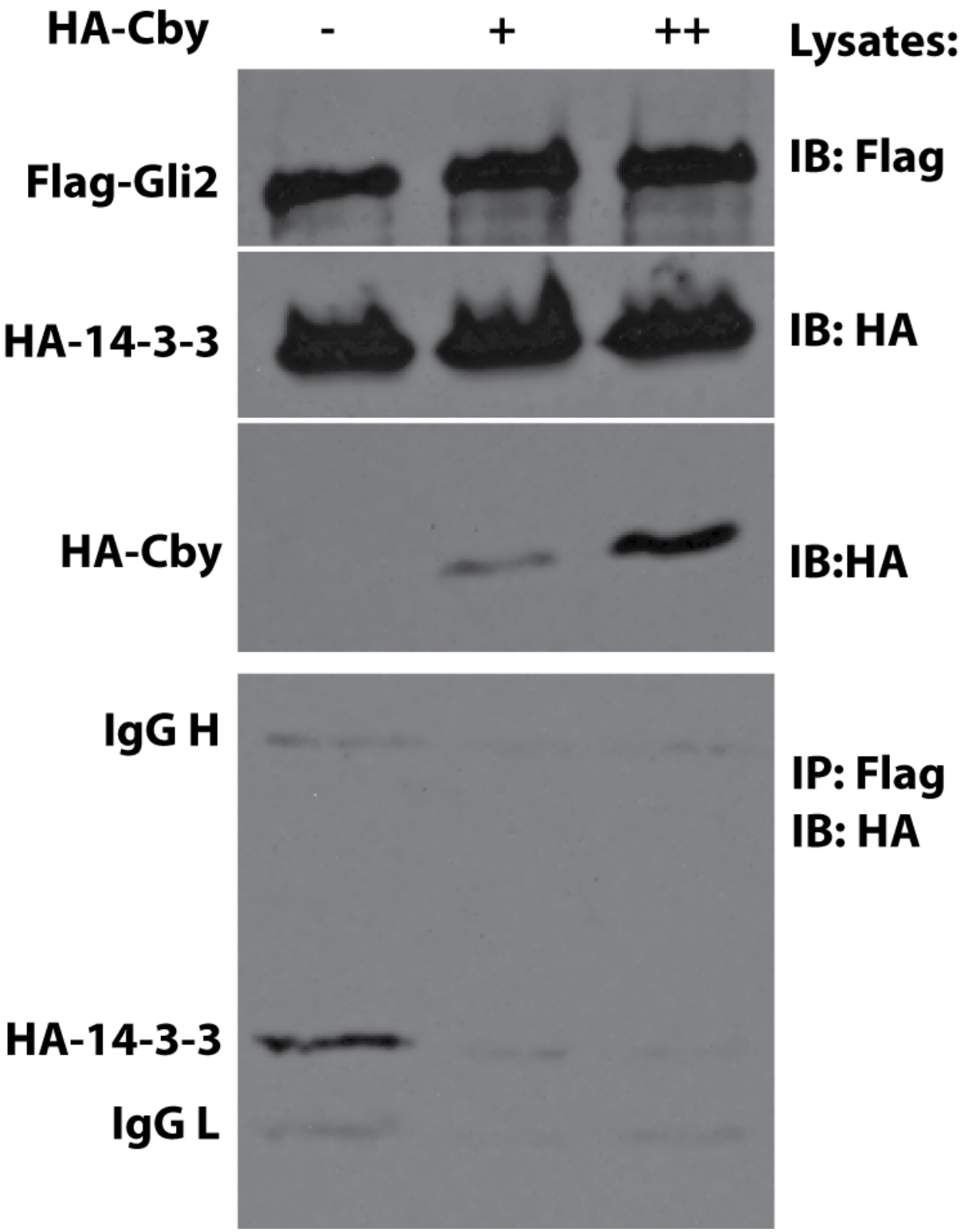

Figure 16: Competition between Cby and 14-3-3 for Gli2 binding

Figure 16: Competition between Cby and 14-3-3 for Gli2 binding:

Co-immunoprecipitation of HA-14-3-3 protein with Flag-Gli2 in the presence of varying concentrations of HA-Cby. (–) denotes absence of HA-Cby, (+) denotes 0.25 ug HA-Cby, and (++) denotes 0.5 ug HA-Cby. Strength of interaction between HA-14-3-3 and Flag-Gli2 and concentration of HA-Cby are inversely proportional to each other, indicating a competition between 14-3-3 and Cby for Gli2 binding.

Chapter 4 Discussion and Future Directions

4.1 A Novel Role for Ciliary Proteins in Zymogen Granule Secretion of Pancreatic Acinar Cells

Pancreatic exocrine degeneration has been associated with aberrant expression of genes known to play vital roles in ciliogenesis and ciliary maintenance (Cano et al, 2004; Cano et al, 2006; Zhang et al, 2004). A number of cases of human ciliopathies have also displayed pancreatic degenerative phenotypes (Chetty-John et al, 2010). This condition has, therefore, been classified as a ciliopathy in these contexts. The mechanism whereby cilia regulate normal exocrine function, and disturbance of these cilia results in defects within this system, remains elusive. In both seminal studies in which exocrine pancreatic degeneration has been definitively associated with aberrant ciliary expression have agreed upon a central dogma, in which pancreatic acinar cells are deleteriously affected in a non-cell autonomous fashion (Cano et al, 2004; Cano et al, 2006; Zhang et al, 2004). The justification for this hypothesis lies in the fact that pancreatic acinar cells do not contain primary cilia (a phenomenon which is attributed to no other pancreatic cells) (Aughsteen, 2001). The mechanism that would support this hypothesis, however, has not been found. The association of ciliopathy patients, as well as these mouse models, with the presence of hyperplastic, and in some cases cystic, pancreatic ducts seems to occur via a much more straightforward mechanism. It seems that loss of cilia in pancreatic ductal cells may result in impairment of fluid flow sensation, similar to what is known of polycystic kidneys in the context of ciliary impairment (Wang & Dong, 2013), and hyperactive Wnt/β-catenin signaling in these cells, resulting in their hyperplastic behavior (Cano et al, 2004; Cano et al, 2006; Zhang et al, 2004). Any connection between this phenotype and degeneration of acinar cells is, at this point, purely speculative.

We show here that Cby-/- mice display rapid and progressive exocrine pancreatic degeneration; very similar to what has been shown in the orpk (Cano et al, 2004; Zhang et al, 2004) and Pdx1-Cre;Kif3a (Cano et al, 2006) mice. At birth, Cby-/- pancreata appear grossly and histologically normal (Fig. 3). Shortly after birth, Cby-/- pancreata display substantial exocrine degeneration, which progresses into adulthood, and is associated with significant lipomatosis (Fig. 1). As well as degeneration of acinar tissue, we show that Cby-/- pancreata display significant ductal hyperplasia (Fig. 2). Unsurprisingly, Cby-/- pancreata also display a marked increase in fibrosis and show definitive signs of chronic inflammation (Fig. 4). These findings, collectively, resulted in the classification of this phenotype as chronic pancreatitis. Cby was found to localize to the base of pancreatic primary cilia (Fig. 5), and there is a reduction in number and length of pancreatic primary cilia in Cby-/- mice (Fig. 6). These data further support the hypothesis that this phenotype, and the potential mechanism of said phenotype, mimics that of orpk and Pdx1-Cre;Kif3a mice, and that this may be a viable model for the pancreatic condition of human ciliopathy patients.

Further characterization of this phenotype was unable to yield a clear rationale for a non-cell autonomous mechanism of pancreatic acinar cell degeneration. As shown in previous models (Cano et al, 2004; Cano et al, 2006; Zhang et al, 2004), there is a significant increase in Wnt/β-catenin signaling in Cby-/- pancreata, which may partially explain the ductal hyperplastic phenotype. Another signaling pathway that is known to be regulated by primary cilia is hedgehog signaling (Goetz & Anderson, 2010). We found that Hh signaling is down-regulated in Cby-/- pancreata through qRT-PCR analysis. Recent studies have shown that hedgehog signaling is necessary for regeneration of injured pancreatic acinar tissue (Cano & Hebrok, 2008). The reduction in hedgehog signaling in Cby-/- pancreata may help explain why exocrine pancreatic

degeneration is so rapidly manifested in these models. Normally, pancreatic degeneration in chronic pancreatitis mouse models takes a significant period of time to be detected (Bombardelli et al, 2010; Hess et al, 2011). This is consistent with the human pathology, which requires numerous bouts of acute pancreatitis before significant damage, and diagnosis of chronic pancreatitis, occurs (Braganza et al, 2011; Stevens et al, 2004). In stark contrast to this, ciliopathy models of pancreatic degeneration, including what is presented here, display significant loss of exocrine tissue almost immediately after mice begin suckling milk.

A closer look at the acinar cells in Cby-/- pancreata revealed that they may possess cell autonomous defects. As early as P0, which is prior to any presence of acinar cell degeneration in Cby-/- pancreata, or either of the other models (Cano et al, 2004; Cano et al, 2006; Zhang et al, 2004), we see that there is a significant disruption in ZG polarity (Fig. 7). This difference in polarity is further manifested by P3, when there is a shift from 100% apically polarized ZGs in wild-type pancreatic acinar cells, to nearly 100% basal in Cby-/- acinar cells (Fig. 7). A closer look at acinar cells by TEM revealed a significant increase in number of ZGs per cell in Cby-/- pancreatic acinar cells, compared with wild-type controls (Fig. 9). This led to the hypothesis that Cby-/- acinar cells were defective in the ability to secrete zymogens, which as further supported by finding a complete loss of zymogen secretion in isolated Cby-/- acinar cells induced with physiologically relevant doses of secretagogue (Fig. 10). This is compared to wild-type controls, which clearly secreted zymogens apically when exposed to the same conditions (Fig. 10). To test whether these acinar cell specific defects were consistent with other models, we obtained tissue from P3 orpk mice, which revealed a similar pattern of disrupted ZG polarity as Cby-/- pancreata (Fig. 8).

While these findings suggested a cell-autonomous defect in pancreatic acinar cells, there still remained a remote possibility that these defects were non-cell autonomous. Analysis of localization patterns of Cby, and a number of other relevant proteins, in pancreatic acinar cells, reduced the likelihood of this possibility. We show that Cby and IFT88 co-localize with ZGs (Fig. 11). IFT20, another member of the anterograde IFTB complex, localizes to both the medial Golgi, and a distinct region overlapping with apically polarized ZGs (Fig. 11). This leads to the hypothesis that intraflagellar transport may play a role in Golgi and vesicle trafficking of pancreatic ZGs. The specificity of ZG localization of these proteins is supported by analysis of purified ZG membranes, in which IFT20, as well as the retrograde IFTA component, IFT140, are present (Fig. 11). The absence of Cby and IFT88 in these samples suggests that they are adjacent, rather than present on ZGs, or their localization to this region is too transient or weak to detect in these harsh conditions. The hypothesis that Cby associates either transiently or weakly with ZGs is supported by evidence of an interaction of Cby and IFT20 (Fig. 11).

Based on data shown here, it seems likely that Cby and IFT88 play a direct role in secretion or trafficking of pancreatic ZGs. Therefore, I hypothesize that it is specific disruption of these proteins, rather than cilia, which results in pancreatic acinar cell degeneration. To test whether there were defects in ZGs themselves, isolated granules of Cby-/- and wild-type pancreatic acinar cells were analyzed by TEM. We show that wild-type granules are present as completely distinct from one another, while Cby-/- ZGs are densely clustered and attached to one another by an unknown electron dense structure (Fig. 12). To test what this structure might be, we submitted samples for mass-spectroscopy. Our preliminary results suggest that actin-related proteins including β-actin are enriched in purified Cby-/- ZGs, which were completely absent from wild-type controls. While this is preliminary and needs further testing, one possibility is

that Cby, potentially in a complex with IFT proteins, regulates ZG trafficking via actin remodeling, and in the absence of Cby, this remodeling is defective, resulting in a dense conglomeration of ZGs and actin fibers, and therefore, and inability to properly traffic and secrete zymogens.

To better understand the mechanism of how Cby may be regulating ZG dynamics, we must determine what the differences between wild-type and Cby-/- ZG membrane content are. While we have preliminary data pointing to a potential accumulation of β-actin on the membranes of Cby-/- ZGs, this route has to be further explored. First, we must be able to detect accumulation of β-actin protein in purified Cby-/- ZGs membranes. If β-actin is present here, and absent in wild-type ZG membranes, we would like to determine if β-actin is present in the unknown electron dense structure seen in purified Cby-/- ZGs. To do this, we plan on performing immuno-electron microscopy, via immuno-gold labeling of β-actin in purified ZGs. We would also like to determine if there are any differences in expression in any other proteins of interest at the ZG membrane, most notably IFT88 and IFT20.

There is growing evidence that intraflagellar transport can regulate non-ciliary vescicle trafficking (Finetti et al, 2014; Sipe & Lu, 2011; Yuan & Sun, 2013). While it is clear that there is a defect in pancreatic acinar cell zymogen secretion in Cby-/- mice, the mechanism, whereby, Cby regulates this process is unclear. The attachment of ZGs to each other indicates that there may be a defect in their fusion or fission. Recently, Cby was found to play a role in vesicle fusion on migrating centrioles during ciliogenesis (Burke et al, Under revision). This suggests that it is more likely that Cby regulates fusion of ZGs. ZG fusion is a critical step in trafficking and secretion. There are two distinct fusion events that occur during ZG secretion. The first of these is the initial fusion of ZGs with the plasma membrane prior to pore formation (Larina et al,

2007; Thorn & Parker, 2005). Following this, subsequent ZGs fuse with the plasma membrane associated ZG, and with each other, forming a chain of ZGs during compound exocytosis (Larina et al, 2007; Thorn & Parker, 2005). Whether there is a defect in either, or both, of these events remains to be tested. Recently, it has been shown that Cby regulates ciliogenesis through regulating of vesicle fusion at migrating mother centrioles (Burke et al, Under revision). Therefore, while our findings are novel, they are not surprising. While there is much work to be done in fully elucidating the mechanism(s) whereby Cby and other ciliary proteins regulate pancreatic ZG trafficking and secretion, this work, and the growing evidence of the true complexity of ciliary biology, should act as a reminder that disorders which manifest themselves out of aberrant ciliary gene expression should not automatically be classified as ciliopathies.

4.2 Cby Plays a Role in Hedgehog Signaling via Regulation of Gli2 Ciliary Trafficking

In mammals, transduction of Hh signaling requires primary cilia (Goetz & Anderson, 2010). In the presence of Hh signaling, Smo is translocated to the tip of primary cilia (Corbit et al, 2005; Wang et al, 2009; Wilson et al, 2009). Along with this, Ptch, which is normally localized along the ciliary axoneme, translocates out of this compartment in the presence of Hh ligand (Rohatgi et al, 2007). Downstream of this, all three mammalian Gli proteins localize to the tip of primary cilia (Haycraft et al, 2005). While this translocation is necessary for activation of Gli2, and loss of repressive function of Gli3 (Haycraft et al, 2005; Jia et al, 2009), the mechanism(s) of how this translocation is regulated is largely unknown.

In the absence of signal, Gli is bound by its negative regulator, Sufu, in the cytoplasm (Zeng et al, 2010). Upon pathway activation, this complex translocates to the tip of the cilium, where Gli dissociates from Sufu and is activated, presumably via interaction with active Smo (Tukachinsky et al, 2010). A known negative regulator of Hh signaling, PKA, is thought to elicit

this regulation in mammals via phosphorylation of the Gli-Sufu complex, which prevents its translocation into the ciliary compartment (Asaoka et al, 2009). More recently, it was found that 14-3-3 protein aids in this negative regulation via interaction with the phosphorylated Gli-Sufu complex (Tukachinsky et al, 2010). This phenomenon displays striking similarity to the known regulation of β-catenin transport out of the nucleus by Cby (Li et al, 2010; Li et al, 2008). Cby forms a complex with β-catenin in the nucleus, and this complex is phosphorylated by Akt (Li et al, 2010). This phosphorylated complex is subsequently bound by 14-3-3 and transported out of the nucleus (Li et al, 2008)

Here we show that Cby, which is known to localize to the base of primary cilia (Lee et al, in press), interacts with all three members of the mammalian Gli transcription factor family. Additionally, loss or reduction of Cby levels in cells containing primary cilia, results in accumulation of Gli2 at the tip of cilia. Based on this and what is known regarding Cby's regulation of Wnt/β-catenin signaling, I hypothesized that Cby may be part of the Gli-Sufu-14-3-3 complex. Contrary to this, we show that Cby seems to compete with 14-3-3 for Gli2 binding. This indicates that Cby may positively, rather than negatively, regulate Hh signaling, as originally speculated. However, this hypothesis requires further testing.

References

Andren-Sandberg A, Hoem D, Gislason H (2002) Pain management in chronic pancreatitis. *Eur J Gastroenterol Hepatol* **14:** 957-970

Asaoka Y, Kanai F, Ichimura T, Tateishi K, Tanaka Y, Ohta M, Seto M, Tada M, Ijichi H, Ikenoue T, Kawabe T, Isobe T, Yaffe MB, Omata M (2009) Identification of a Suppressive Mechanism for Hedgehog Signaling through a Novel Interaction of Gli with 14-3-3. *Journal of Biological Chemistry* **285:** 4185-4194

Aughsteen A (2001) The Ultrastructure of Primary Cilia in the Endocrine and Excretory Duct Cells of the Pancreas of Mice and Rats. *Eur J Morphol* **39:** 277-283

Badano J, Mitsuma N, Beales P, Katsanis N (2006) The ciliopathies: an emerging class of human genetic disorders. *Annu Rev Genomics Hum Genet* **7:** 125-148

Bardeesy N, DePinho RA (2002) Pancreatic cancer biology and genetics. *Nature Reviews Cancer* **2:** 897-909

Bettencourt-Dias M, Hildebrandt F, Pellman D, Woods G, Godinho SA (2011) Centrosomes and cilia in human disease. *Trends in Genetics* **27:** 307-315

Bishop CL, Bergin A-MH, Fessart D, Borgdorff V, Hatzimasoura E, Garbe JC, Stampfer MR, Koh J, Beach DH (2010) Primary Cilium-Dependent and -Independent Hedgehog Signaling Inhibits p16INK4A. *Molecular Cell* **40:** 533-547

Bombardelli L, Carpenter ES, Wu AP, Alston N, DelGiorno KE, Crawford HC (2010) Pancreas-Specific Ablation of β1 Integrin Induces Tissue Degeneration by Disrupting Acinar Cell Polarity. *Gastroenterology* **138:** 2531-2540.e2534

Braganza JM, Lee SH, McCloy RF, McMahon MJ (2011) Chronic Pancreatitis. *Lancet* **377:** 1184-1197

Briscoe J, Therond P (2013) The mechanisms of Hedgehog signalling and its roles in development and disease. *Nat Re Mol Cell Biol* **14:** 416-429

Brock C, Nielsen L, Lelic D, Drewes A (2013) Pathophysiology of chronic pancreatitis. *World Journal of Gastroenterology* **19:** 7231-7240

Burke M, Li FQ, Cyge B, Arashiro T, Brechbuhl HM, O'Connell CB, Weiss M, Chen X, Love D, Brody SL, Westlake C, Reynolds SD, Kuriyama R, Takemaru KI (Under revision) Basal Body Docking Requires Chibby-Mediated Ciliary Vesicle Formation during Airy Ciliated Cell Differentiation.

Callejo A, Culi J, Guerrero I (2008) Patched, the receptor of Hedgehog, is a lipoprotein receptor. *Proceedings of the National Academy of Sciences* **105:** 912-917

Cano D, Murcia N, Pazour G, Hebrok M (2004) Orpk mouse model of polycystic kidney disease reveals essential role of primary cilia in pancreatic tissue organization. *Development* **131:** 3457-3467

Cano D, Sekine S, Hebrok M (2006) Primary Cilia Deletion in Pancreatic Epithelial Cells Results in Cyst Formation and Pancreatitis. *Gastroenterology* **131:** 1856-1869

Cano DA, Hebrok M (2008) Hedgehog Spikes Pancreas Regeneration. *Gastroenterology* **135:** 347-351

Cavallini G, Talamini G, Vaona B, Bovo P, Filippini M, Rigo L, Angelini G, Vantini I, Riela A, Frulloni L (1994) Effect of alcohol and smoking on pancreatic lithogenesis in the course of chronic pancreatitis. *Pancreas* **9:** 42-46

Cervantes S, Lau J, Cano DA, Borromeo-Austin C, Hebrok M (2010) Primary cilia regulate Gli/Hedgehog activation in pancreas. *Proceedings of the National Academy of Sciences* **107:** 10109-10114

Chen Y, Yue S, Xie L, Pu Xh, Jin T, Cheng SY (2011) Dual phosphorylation of Suppressor of fused by PKA and GSK3beta regulates its stability and localization in the primary cilium. *Journal of Biological Chemistry* **286:** 13502-13511

Chetty-John S, Piwnica-Worms K, Bryant J, Bernardini I, Fischer RE, Heller T, Gahl WA, Gunay-Aygun M (2010) Fibrocystic disease of liver and pancreas; under-recognized features of the X-linked ciliopathy oral-facial-digital syndrome type 1 (OFD I). *American Journal of Medical Genetics Part A* **152A:** 2640-2645

Cole D, Diener D, Himelblau A, Beech P, Fuster J, Rosenbaum J (1998) Chlamydomonas kinesin-II-dependent intraflagellar transport (IFT): IFT particles contain proteins required for ciliary assembly in Caenorhabditis elegans sensory neurons. *J Cell Biol* **141:** 993-1008

Corbit K, Aanstad P, Singla V, Norman A, Stainier D, Reiter J (2005) Vertebrate Smoothened functions at the primary cilium. *Nature* **437:** 1018-1021

Corcoran R, Scott M (2006) Oxysterols stimulate Sonic hedgehog signal transduction and proliferation of medulloblastoma cells. *Proceedings of the National Academy of Sciences* **103:** 8408-8413

Cosen-Binker LI, Binker MG, Wang C-C, Hong W, Gaisano HY (2008) VAMP8 is the v-SNARE that mediates basolateral exocytosis in a mouse model of alcoholic pancreatitis. *Journal of Clinical Investigation* **118:** 2535-2551

Cosen–Binker LI, Lam PPL, Binker MG, Gaisano HY (2007) Alcohol-Induced Protein Kinase Cα Phosphorylation of Munc18c in Carbachol-Stimulated Acini Causes Basolateral Exocytosis. *Gastroenterology* **132:** 1527-1545

Denef N, Neubuser D, Perez L, Cohen S (2000) Hedgehog induces opposite changes in turnover and subcellular localization of patched and smoothened. *Cell* **102:** 521-531

Dwyer J, Sever N, Carlson M, Nelson S, Beachy P, Parhami F (2007) Oxysterols are novel activators of the hedgehog signaling pathway in pluripotent mesenchymal cells. *J Biol Chem* **23:** 8959-8968

EK V, Brody SL (2013) Analysis of ciliogenesis in primary cultrue mouse tracheal epithelial cells. *Methods Enzymol* **525:** 285-309

Enjolras C, Thomas J, Chhin B, Cortier E, Duteyrat JL, Soulavie F, Kernan MJ, Laurencon A, Durand B (2012) Drosophila chibby is required for basal body formation and ciliogenesis but not for Wg signaling. *The Journal of Cell Biology* **197:** 313-325

Finetti F, Patrussi L, Masi G, Onnis A, Galgano D, Luscherini OM, Pazour GJ, Baldari CT (2014) Immune synapse targeting of specific recycling receptors by the intraflagellar transport system. *Journal of Cell Science* **127:** 1924-1937

Gailani M, Stahle-Backdahl M, Leffell D, Glynn M, Zaphiropoulos P, Pressman C, Unden A, Dean M, Brash D, Bale A, Toftgard R (1996) The role of the human homologue of Drosophila patched in sporadic basal cell carcinomas. *Nat Genet* **14:** 78-81

Gardner T, Kennedy A, Gelrud A, Banks P, Vege S, Gordon S, Lacy B (2010) Chronic pancreatitis and its effect on employment and health care experience: results of a prospective American multicenter study. *Pancreas* **39:** 498-501

Gerdes JM, Davis EE, Katsanis N (2009) The Vertebrate Primary Cilium in Development, Homeostasis, and Disease. *Cell* **137:** 32-45

Goetz SC, Anderson KV (2010) The primary cilium: a signalling centre during vertebrate development. *Nature Reviews Genetics* **11:** 331-344

Grendell J (1983) Nutrition and absorption in diseases of the pancreas. *Clin Gastroenterol* **12:** 551-562

Haycraft CJ, Banizs B, Aydin-Son Y, Zhang Q, Michaud EJ, Yoder BK (2005) Gli2 and Gli3 Localize to Cilia and Require the Intraflagellar Transport Protein Polaris for Processing and Function. *PLoS Genetics* **preprint:** e53

Heretsch P, Tzagkaroulaki L, Giannis A (2010) Modulators of the hedgehog signaling pathway. *Bioorganic & Medicinal Chemistry* **18:** 6613-6624

Hess DA, Humphrey SE, Ishibashi J, Damsz B, Lee AH, Glimcher LH, Konieczny SF (2011) Extensive Pancreas Regeneration Following Acinar-Specific Disruption of Xbp1 in Mice. *Gastroenterology* **141:** 1463-1472

Hooper J, Scott M (1989) The Drosophila patched gene encodes a putative membrane protein required for segmental patterning. *Cell* **59:** 751-765

Huangfu D, Liu A, Rakeman A, Murcia N, Niswander L, Anderson K (2003) Hedgehog signaling in the mouse requires intraflagellar transport proteins. *Nature* **426:** 83-87

Hui C, Angers S (2011) Gli proteins in development and disease. *Annu Rev Cell Dev Biol* **27:** 513-537

Humke E, Dorn K, Milenkovic L, Scott M, Rohatgi R (2010) The output of Hedgehog signaling is controlled by the dynamic association between Supressor of Fused and The Gli proteins. *Genes Dev* **24:** 670-682

Ingham P, McMahon A (2001) Hedgehog signaling in animal development: paradigms and principles. *Genes & Development* **15:** 3059-3087

Ingham P, Nakano Y, Seger C (2011) Mechanisms and functions of Hedgehog signalling across the metazoa. *Nat Rev Genet* **12:** 393-406

Jia J, Kolterud A, Zeng H, Hoover A, Teglund S (2009) Suppressor of Fused inhibits mammalian Hedgehog signaling in the absence of cilia. *Dev Biol* **330:** 452-460

Jiang J, Hui C (2008) Hedgehog signaling in development and cancer. *Dev Cell* **15:** 801-812

Kayed H, Kleef J, Osman T, Shereen K, Buckler MW, Friess H (2006) Hedgehog Signaling in the Normal and Diseased Pancreas. *Pancreas* **32:** 119-129

Keady Brian T, Samtani R, Tobita K, Tsuchya M, San Agustin Jovenal T, Follit John A, Jonassen Julie A, Subramanian R, Lo Cecilia W, Pazour Gregory J (2012) IFT25 Links the Signal-Dependent Movement of Hedgehog Components to Intraflagellar Transport. *Developmental Cell* **22:** 940-951

Kloppel G, Detlefsen S, Feyerabend B (2004) Fibrosis of the pancreas: the initial tissue damage and the resulting pattern. *Virchows Archiv* **445:** 1-8

Kuhlmann K, Tschapek A, Wiese H, Eisenacher M, Meyer HE, Hatt HH, Oeljeklaus S, Warscheid B (2014) The Membrane Proteome of Sensory Cilia to the Depth of Olfactory Receptors. *Molecular and Cellular Proteomics* **13:** 1828-1843

Lancaster MA, Schroth J, Gleeson JG (2011) Subcellular spatial regulation of canonical Wnt signalling at the primary cilium. *Nature Cell Biology* **13:** 702-709

Larina O, Bhat P, Pickett JA, Launikonis BS, Shah A, Kruger WA, Edwardson JM, Thorn P (2007) Dynamic Regulation of the Large Exocytotic Fusion Pore in Pancreatic Acinar Cells. *Molecular Biology of the Cell* **18:** 3502-3511

Lee L (2011) Mechanisms of mammalian ciliary motility: Insights from primary ciliary dyskinesia genetics. *Gene* **473:** 57-66

Lee RJ, Cohen NA (2013) The emerging role of the bitter taste receptor T2R38 in upper respiratory infection and chronic rhinosinusitis. *American Journal of Rhinology and Allergy* **27:** 283-286

Lee Y-L, Sante J, Comerci CJ, Cyge B, Menezes LF, Li F-Q, Germino GG, Moerner WE, Takemaru K-I, Stearns T (in press) Cby1 promotes Ahi1 recruitment to a ring-shaped domain at the centriole-cilium interface and facilitates proper cilium formation and function. *Molecular Biology of the Cell*

Levy P, Mathurin P, Roqueplo A, Rueff B, Bernades P (1995) A multidimensional case-control study of dietary, alcohol, and tobacco habits in alcoholic men with chronic pancreatitis. *Pancreas* **10:** 231-238

Li F, Mofunanya A, Fischer V, Hall J, Takemaru KI (2010) Nuclear-cytoplasmic shuttling of Chibby controls beta-catenin signaling. *Mol Biol Cell* **21:** 311-322

Li F, Mofunanya A, Harris K, Takemaru KI (2008) Chibby cooperates with 14-3-3 to regulate beta-catenin subcellular distribution and signaling activity. *J Cell Biol* **181:** 1141-1154

Li S, Chen Y, Shi Q, Yue T, Wang B, Jiang J (2012) Hedgehog-regulated ubiquitination controls smoothened trafficking and cell surface expression in Drosophila. *PLoS Biology* **10:** e1001239

Lindemann C, Lesich K (2010) Flagellar and ciliary beating: the proven and the possible. *J Cell Sci* **123:** 519-528

Litingtung Y, Chiang C (2000) Specification of ventral neuron types is mediated by an antagonistic interaction between Shh and Gli3. *Nat Neurosci* **3:** 979-985

Love D, Li F-Q, Cyge B, Burke MC, Ohmitsu M, Cabello J, Larsen JE, Brody SL, Cohen JC, Takemaru K-I (2010) Altered Lung Morphogenesis, Epithelial Cell Differentiation and Mechanics in Mice Deficient in the Wnt/b-Catenin Antagonist Chibby. *PloS ONE* **5:** e13600

Matise M, Epstein D, Park H, Platt K, Joyner A (1998) Gli2 is required for induction of floor plate and adjacent cells, but not most ventral neurons in mouse central nervous system. *Development* **125:** 2759-2770

Mofunanya A, Li F, Hsieh J, Takemaru KI (2009) Chibby forms a homodimer through a heptad repeat of leucine residues in its C-terminal coiled-coil motif. *BMC Mol Biol* **10:** 41

Nakano Y, Guerrero I, Hidalgo A, Taylor A, Whittle J, Ingham P (1989) A protein with several possible membrane-spanning domains encoded by the Drosophila segment polarity gene patched. *Nature* **341:** 508-513

Nauli SM, Jin X, AbouAlaiwi WA, El-Jouni W, Su X, Zhou J (2013) Non-Motile Primary Cilia as Fluid Shear Stress Mechanosensors. *Methods Enzymol* **525:** 1-20

Nielsen SK, Møllgård K, Clement CA, Veland IR, Awan A, Yoder BK, Novak I, Christensen ST (2008) Characterization of primary cilia and Hedgehog signaling during development of the human pancreas and in human pancreatic duct cancer cell lines. *Developmental Dynamics* **237:** 2039-2052

Nusslein-Volhard C, Wieschaus E (1980) Mutations affecting segment number and polarity in Drosophila. *Nature* **287:** 795-801

Oh EC, Katsanis N (2012) Context-Dependent Regulation of Wnt Signaling through the Primary Cilium. *Journal of the American Society of Nephrology* **24:** 10-18

Olesen A, Brokjaer A, Fisher I, Larsen I (2013) Pharmacological challenges in chronic pancreatitis. *World Journal of Gastroenterology* **19:** 7302-7307

Orozco J, Wedaman K, Signor D, Brown H, Rose L, Scholey J (1999) Movement of motor and cargo along cilia. *Nature* **398:** 674

Park H, Bai C, Platt K, Matise M, Beeghly A, Hui C, Nakashima M, Joyner A (2000) Mouse Gli1 mutants are viable but have defects in SHH signaling in combination with a Gli2 mutation. *Development* **127:** 1593-1605

Pazour GJ, Dickert BL, Vucica Y, Seeley ES, Rosenbaum JL, Witman GB, Cole DG (2000) Chlamydomonas IFT88 and Its Mouse Homologue, Polycystic Kidney Disease Gene Tg737, Are Required for Assembly of Cilia and Flagella. *Journal of Cell Biology* **151:** 709-718

Philipps R (1981) The airway mucociliary system. *Int Rev Physiol* **23:** 213-260

Raimondi S, Lowenfels A, Morselli-Labate A, Maisonneuve P, Pezzili R (2010) Pancreatic cancer in chronic pancreatitis; aetiology, incidence, and early detection. *Best Pract Res Clin Gastroenterol* **24:** 349-358

Rohatgi R, Milenkovic L, Scott M (2007) Patched1 regulates hedgehog signaling at the primary cilium. *Science* **317:** 372-376

Rosenbaum J, Moulder J, Ringo D (1969) Flagellar elongation and shortening in Chlamydomona. The use of cycloheximide and colchicine to study the synthesis and assembly of flagellar proteins. *J Cell Biol* **41:** 600-619

Rosenbaum J, Witman G (2002) Intraflagellar transport. *Nat Rev Mol Cell Biol* **3:** 813-825

Rovira M, Scott SG, Liss AS, Jensen J, Thayer SP, Leach SD (2009) Isolation and characterization of centroacinar/terminal ductal progenitor cells in adult mouse pancreas. *Proceedings of the National Academy of Sciences* **107:** 75-80

Satir P (1965) STUDIES ON CILIA : II. Examination of the Distal Region of the Ciliary Shaft and Role of the Filaments in Motility. *J Cell Biol* **26:** 805-834

Satir P, Christensen ST (2008) Structure and function of mammalian cilia. *Histochemistry and Cell Biology* **129:** 687-693

Scales S, de Sauvage F (2009) Mechanisms of Hedgehog pathway activation in cancer and implications for therapy. *Trends in Pharmacol Sci* **30:** 303-312

Schneider A, Lohr J, Singer M (2007) The M-ANNHEIM classification of chronic pancreatitis: introduction of a unifying classification system based on a review of previous classifications of the disease. *Journal of Gastroenterology* **42:** 101-119

Schneider A, Pfutzer R, Witcomb D (2002) Genetics and pancreatic disease. *Curr Opin Gastroenterol* **18:** 545-551

Scholey J (2008) Intraflagellar transport motors in cilia: moving along the cell's antenna. *J Cell Biol* **180:** 23-29

Sipe CW, Lu X (2011) Kif3a regulates planar polarization of auditory hair cells through both ciliary and non-ciliary mechanisms. *Development* **138:** 3441-3449

Slade I, Murray A, Hanks S, Kumar A, Walker L, Hargrave D, Douglas J, Stiller C, Izatt L, Rahman N (2011) Heterogeneity of familial medulloblastoma and contribution of germline PTCH1 and SUFU mutations to sporadic medulloblastoma. *Fam Cancer* **10:** 337-342

Steere N, Chae V, Burke M, Li F-Q, Takemaru K-I, Kuriyama R (2012) A Wnt/beta-Catenin Pathway Antagonist Chibby Binds Cenexin at the Distal End of Mother Centrioles and Functions in Primary Cilia Formation. *PLoS ONE* **7:** e41077

Stevens T, Conwell DL, Zuccaro G (2004) Pathogenesis of chronic pancreatitis: An evidence-based review of past theories and recent developments. *Am J Gastroenterol* **99:** 2256-2270

Sung C-H, Leroux MR (2013) The roles of evolutionarily conserved functional modules in cilia-related trafficking. *Nature Cell Biology* **15:** 1387-1397

Takemaru K-I, Yamaguchi S, Lee YS, Zhang Y, Carthew RW, Moon RT (2003) Chibby, a nuclear b-catenin associated antagonist of the Wnt/Wingless pathway. *Nature* **422:** 905-909

Taylor M, Liu L, Raffel C, Hui C, Mainprize T, Zhang X, Agatep R, Chiappa S, Gao L, Lowrance A, Hao A, Goldstein A, Stavrou T, Scherer S, Dura W, Wainwright B, Squire J, Rutka J, Hogg D (2002) Mutations in SUFU predispose to medulloblastoma. *Nat Genet* **31:** 306-310

Teglund S, Toftgard R (2010) Hedgehog beyond medulloblastoma and basal cell carcinoma. *Biochim Biophys Acta* **1805:** 181-208

Thorn P, Parker I (2005) Two phases of zymogen granule lifetime in mouse pancreas: ghost granules linger after exocytosis of contents. *J Physiol* **563:** 433-442

Tukachinsky H, Lopez LV, Salic A (2010) A mechanism for vertebrate Hedgehog signaling: recruitment to cilia and dissociation of SuFu-Gli protein complexes. *The Journal of Cell Biology* **191:** 415-428

Tuson M, He M, Anderson KV (2011) Protein kinase A acts at the basal body of the primary cilium to prevent Gli2 activation and ventralization of the mouse neural tube. *Development* **138:** 4921-4930

Uscanga L, Robles-Diaz G, RAmirez J, Campuzano Fernandez M (1985) Clinical significance of pancreas divisum. *Rev Gastroenterol Mex* **50:** 169-174

van Asselt SJ, de Vries EG, van Dulleman HM, Brouwers AH, Walenkamp AM, Giles RH, Links TP (2013) Pancreatic cyst development: insights from von Hippel-Lindau disease. *Cilia* **2:** 3

van Reeuwijk J, Arts HH, Roepman R (2011) Scrutinizing ciliopathies by unraveling ciliary interaction networks. *Human Molecular Genetics* **20:** R149-R157

Villavicencio EH, Walterhouse DO, Iannaccone PM (2000) The Sonic Hedgehog-Patched-Gli Pathway in Human Development and Disease. *Am J Hum Genet* **67:** 1047-1054

Voronina VA, Takemaru KI, Treuting P, Love D, Grubb BR, Hajjar AM, Adams A, Li FQ, Moon RT (2009) Inactivation of Chibby affects function of motile airway cilia. *The Journal of Cell Biology* **185:** 225-233

Wagner ACC, Strowski MZ, Williams JA (1994) Identification of rab 5 but not rab 3a in rat pancreatic zymogen granule membranes. *Biochemical and Biophysical Research Communications***:** 542-548

Wang S, Dong Z (2013) Primary cilia and kidney injury: current research status and future perspectives. *Am J Physiol Renal Physiol* **305:** F1085-F1098

Wang Y, Zhou Z, Walsh C, McMahon A (2009) Selective translocation of intracellular Smoothened to the primary cilium in response to Hedgehog pathway modulation. *Proceedings of the National Academy of Sciences* **106:** 2623-2628

Warren K, Murray M (2013) Alcoholic liver disease and pancreatitis: global health problems being addressed by the US National Institute on Alcohol Abuse and Alcoholism. *J Gastroenterol Hepatol* **28:** 4-6

Warshaw A, Banks P, Fernandez-Del Castillo C (1998) AGA technical review: treatment of pain in chronic pancreatitis. *Gastroenterology* **115:** 765-776

Waters AM, Beales PL (2011) Ciliopathies: an expanding disease spectrum. *Pediatric Nephrology* **26:** 1039-1056

Wheway G, Parry DA, Johnson CA (2013) The role of primary cilia in development and disease of the retina. *Organogenesis* **10:** 69-85

Williams CL, Li C, Kida K, Inglis PN, Mohan S, Semenec L, Bialas NJ, Stupay RM, Chen N, Blacque OE, Yoder BK, Leroux MR (2011) MKS and NPHP modules cooperate to establish basal body/transition zone membrane associations and ciliary gate function during ciliogenesis. *The Journal of Cell Biology* **192:** 1023-1041

Wilson CW, Chen M, Chuang P (2009) Smoothened adopts multiple active and inactive conformations capable of trafficking to the primary cilium. *PLoS ONE* **4:** e5182

Yamamoto M, Kataoka K (1986) Electron microscopic observation of the primary cilium in the pancreatic islets. *Arch Histrol Jpn* **49:** 449-457

Yonezawa S, Higashi M, Yamada N, Goto M (2008) Precursor lesions of pancreatic cancer. *Gut Liver* **2:** 137-154

Yuan S, Sun Z (2013) Expanding Horizons: Ciliary Proteins Reach Beyond Cilia. *Annual Review of Genetics* **47:** 353-376

Zeng H, Jia J, Liu A (2010) Coordinated translocation of mammalian Gli proteins and suppressor of fused to the primary cilium. *PLoS ONE* **5:** e15900

Zhang Q, Davenport JR, Croyle MJ, Haycraft CJ, Yoder BK (2004) Disruption of IFT results in both exocrine and endocrine abnormalities in the pancreas of Tg737orpk mutant mice. *Laboratory Investigation* **85:** 45-64